8-7-2024

AI-based methods for detecting and classifying age-related macular degeneration: a comprehensive review

Niveen Nasr El-Den
Ain Shams University

Mohamed Elsharkawy
University of Louisville

Ibrahim Saleh
University of Maryland, Baltimore

Mohammed Ghazal
Abu Dhabi University

Ashraf Khalil
Zayed University, ashraf.khalil@zu.ac.ae

See next page for additional authors

Artificial Intelligence Review (2024) 57:237
https://doi.org/10.1007/s10462-024-10883-3

AI-based methods for detecting and classifying age-related macular degeneration: a comprehensive review

Niveen Nasr El-Den[1] · Mohamed Elsharkawy[2] · Ibrahim Saleh[3] · Mohammed Ghazal[4] · Ashraf Khalil[5] · Mohammad Z. Haq[6] · Ashraf Sewelam[7] · Hani Mahdi[1] · Ayman El-Baz[2]

Accepted: 25 July 2024

Abstract
This paper explores the advancements and achievements of artificial intelligence (AI) in computer vision (CV), particularly in the context of diagnosing and grading age-related macular degeneration (AMD), one of the most common leading causes of blindness and low vision that impact millions of patients globally. Integrating AI in biomedical engineering and healthcare has significantly enhanced the understanding and development of the CV application to mimic human problem-solving abilities. By leveraging AI-based models, ophthalmologists can improve the accuracy and speed of disease diagnosis, enabling early treatment and mitigating the severity of the conditions. This paper presents a comprehensive analysis of many studies on AMD published between 2014 and 2024, with more than 80% published after 2020. Various methodologies and techniques are examined, particularly emphasizing utilizing different retinal imaging modalities like color fundus photography and optical coherence tomography (OCT), where 66% of the studies used OCT datasets. This review aims to compare the efficacy of these AI-based approaches, including machine learning and deep learning, in detecting and diagnosing different stages and grades of AMD based on the evaluation of different performance metrics using different private and public datasets. In addition, this paper introduces some suggested AI solutions for future work.

Keywords Age-related macular degeneration · Artificial intelligence · Color Fundus Photography · Deep learning · Machine learning · Optical coherence tomography

✉ Ayman El-Baz
aselba01@louisville.edu

[1] Department of Computer and System Engineering, Faculty of Engineering, Ain Shams University, Cairo 11517, Egypt

[2] Department of Bioengineering, University of Louisville, Louisville, KY 40292, USA

[3] Department of Ophthalmology and Visual Sciences, University of Maryland School of Medicine, Baltimore, MD, USA

[4] Electrical and Computer Engineering Department, Abu Dhabi University, Abu Dhabi 59911, UAE

[5] College of Technological Innovation, Zayed University, 4783 Abu Dhabi, UAE

[6] School of Medicine, University of Louisville, Louisville, KY 40292, USA

[7] Ophthalmology Department, Faculty of Medicine, Mansoura University, Mansoura, Egypt

1 Introduction

Artificial intelligence (AI) and its sub-fields are rapidly expanding, playing a crucial role with significant implications. They are revolutionizing many sectors and driving innovation and advancement across various fields, from everyday routines to cutting-edge developments. AI-based technologies are becoming integral to our daily activities and are transforming everything from our routine tasks to complex professional endeavors. Notable progress has been recorded in areas such as self-driving cars (Caleffi et al. 2024), physics and dynamics (Bilal and Sun 2020; Raja et al. 2019), farming and agriculture (Attri et al. 2024; Bilal et al. 2023; Vani et al. 2023).

In the biomedical sector, AI-based models analyze genetic data and improve gene imputation spot (Arisdakessian et al. 2019; Feng et al. 2024), identify DNA methylation (Bai et al. 2023; Yu et al. 2024; Zheng et al. 2023) that is important to regulating gene expression without changing the DNA sequence. In the healthcare sector, they automatically detect and diagnose diseases and identify disease risks, improving clinical service quality, patient satisfaction, and medical resource efficiency (Lee and Lee 2020; Yoon and Lee 2018), such as detecting lung cancer (Bilal et al. 2022a, b; Elsharkawy et al. 2021; Hussain Ali et al. 2023; Naseer et al. 2023; Suresh and Mohan 2022), breast cancer (Almutairi et al. 2023; Bilal et al. 2024a, b; Elkorany and Elsharkawy 2023; Elkorany et al. 2022), skin cancer (Alam et al. 2022), recognition of finger vein (Bilal et al. 2021), HIV infection (Bilal et al. 2021; Sabir et al. 2024; Umar et al. 2021), diabetic retinopathy (DR) (Anoop 2022; Bilal et al. 2021; Bilal et al. 2022; Bilal et al. 2024a, b; Elsharkawy et al. 2022a, b; Khan et al. 2024; Mohan et al. 2023; Sandhu et al. 2020; Sharafeldeen et al. 2021), classifying vision-threatening diabetic retinopathy (VTDR) (Bilal et al. 2023; Bellemo et al. 2019; Ipp et al. 2021), where AI outperforms human clinical specialists in detecting and diagnosing different diseases, allowing for earlier treatment and prevention of disease progression.

Traditionally, detecting and diagnosing retinal disorders clinically involves patient screening, recording their medical history, examining their eyes, and evaluating medical imaging such as Color Fundus Photography (CFP), optical coherence tomography (OCT), and spectral domain optical coherence tomography (SD-OCT). The clinical decision is based on the doctor's analytical conclusion after assessing the imaging exams, which is subject to human interpretation. Finally, the doctor recommends a specific prescription to the patient based on their condition. Figure 1 shows an overview of traditional detecting and diagnosing retinal disorders.

Machine learning (ML) (Mahmoudi et al. 2021) is a sub-field of AI where the machine learns how to imitate human behavior (Ongsulee 2017). It plays a vital role and already has a significant impact on healthcare research using medical imaging. Particularly, imaging technologies such as CFP, fundus auto-fluorescence imaging, OCT supplemented by fluorescein angiography, and OCT angiography (OCTA) without requiring any dye injection have improved the ability to identify and diagnose retinal disorders (Ferris III et al. 2013). ML trains machines to develop their intelligence by learning from large amounts of collected data without being explicitly programmed (Carbonell et al. 1983). The growing demand for tools that can assist doctors in diagnosing and treating patients more effectively, along with the availability of medical imaging devices and ML, has spurred the development of health-related AI applications in healthcare research areas that were previously believed to be only detected by human experts (Lee and Yoon 2021).

Vision is a crucial human sense, as the predominant source of information we receive is acquired through visual perception. Retinal disorders are well-known causes of vision

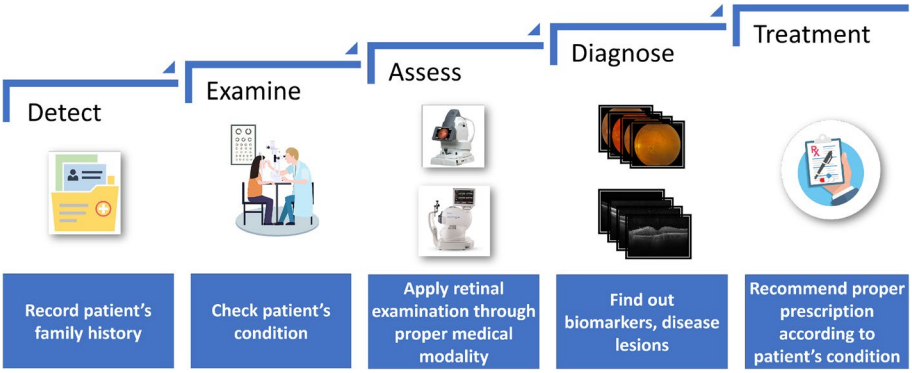

Fig. 1 An illustrative figure for the flow diagram of the traditional steps for diagnosing and grading retinal diseases

impairment and blindness; they have sparked countless studies and investigations. In 2020, cataract, glaucoma, under-corrected refractive error, age-related macular degeneration (AMD), and DR were the top five main causes of visual impairment that may lead to complete vision loss in the world (Bourne et al. 2021; Elsharkawy et al. 2022; Haggag et al. 2022; Lim et al. 2012; Sleman et al. 2021; Steinmetz et al. 2021).

In the literature, ML approaches, including deep learning (DL) and transfer learning (TL) techniques, for producing powerful AI models that simulate human physiology have recorded significant successes in detecting retinal diseases and classifying grades of severity. DL, as a subset of ML, is an approach that mimics the human visual system by using multiple layers of convolutional neural networks (CNNs). It has been widely used for various CV applications due to its capability of identifying patterns in images. TL techniques use a pre-trained model to solve a new problem. This includes transferring knowledge from the selected pre-trained model to a medical imaging domain rather than starting the learning process from scratch, which results in accelerating the training of new models and reducing computational resources. Figure 2 shows an overview of disease classification and lesion detection utilizing any of the AI-based approaches, starting by inputting any image modalities to the chosen AI approach, where the model can either recognize the given disease's various grades or determine whether the disease occurred or not. The input is one of many different image modalities, such as fundus and OCT images, where both have been utilized in the detection and identification of different retinal disorders such as AMD and DR. According to the trained model, the output is either binary classification, where the model can distinguish between a normal and affected retina, or multi-way classification, where the model can identify the various grades of the disease. DL-based models have demonstrated their capabilities in different medical domains for data analysis, segmentation, automated diagnosis, and potential result prediction (Chan et al. 2020; Elsharkawy et al. 2023).

Our primary goal is to compare different models and systems that use different AI approaches and techniques to detect and classify AMD based on medical imaging, such as CFP and OCT, to help understand AI-based models' future role in retinal disorder diagnoses, especially AMD, and their significant impact on enhancing patient's life quality and halting disease progression. Moreover, other retinal disorders leading to blindness typically require further examinations to confirm the diagnosis. We compiled tables summarizing

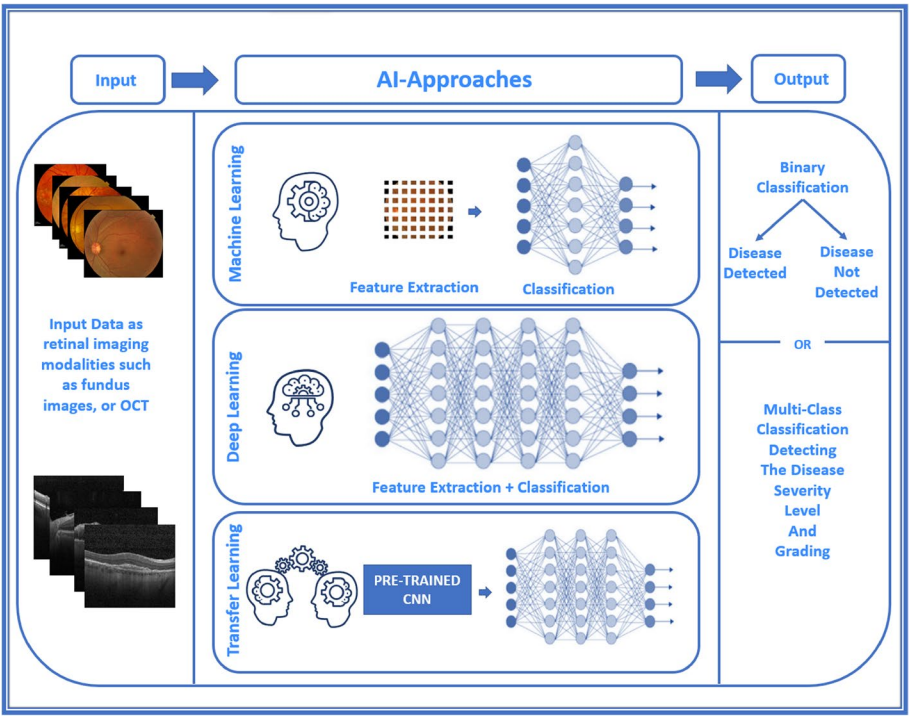

Fig. 2 An illustrative figure for the flow diagram of any CAD system for diagnosing and grading retinal diseases

the detection and classification of different grades of AMD using various imaging modalities. These tables include key details such as the first author of each study, the year of publication, the methods and techniques employed, performance evaluations, relevant metrics like accuracy, the datasets used for training and testing, and the advantages and limitations of the proposed models.

In this paper, we present a comprehensive survey of recent research on the detection and diagnosis of AMD using CFP and OCT. We analyze and discuss the advancements in CAD systems, evaluating their impact on patient well-being by examining their advantages and limitations. Furthermore, we offer clear recommendations for future research directions, aiming to inspire academic studies and practical initiatives. Additionally, we propose alternative methodologies and approaches to advance the field of AMD diagnosis, leveraging the potential of CFP, OCT, and OCTA technologies to enhance diagnostic accuracy and patient care.

This paper is organized as follows: in section Age-related Macular Degeneration, we introduce the prevalence and the statistical analysis of AMD, its pathophysiology and grading, different imaging modalities and diagnosis, AI approaches, and datasets used. The literature works related to AMD detection and grading are presented in section AMD Detection and Classification Approaches, showing the AI-based approaches used for diagnosing and distinguishing between its grades. The discussion and future directions are discussed in section Discussion and section Future Direction, respectively. The conclusion is presented in section Conclusion.

2 Age-related macular degeneration

AMD is the leading cause of irreversible blindness in developed countries, particularly in people over the age of 60 (Gehrs et al. 2006; Wong et al. 2014). AMD develops due to the dynamic interrelationship between the aging process, genetic predisposition, and diverse environmental risk factors such as smoking (Fleckenstein et al. 2021).

AMD affects the macula, the central part of the retina, a thin layer of tissue lining the inside wall of the back of the eye (Apte 2021; Hobbs and Pierce 2022). Early detection of AMD is essential for controlling its progression and complications, permitting a faster start to treatment and thus improving the overall prognosis (Schwartz and Loewenstein 2015). AMD grades can be determined by the quantity and size of drusen, defined as yellow retinal deposits, and the presence of other retinal abnormalities, as shown in Table 1. AMD is diagnosed and monitored using various imaging techniques, including fundus images that help in detecting retinal abnormalities such as drusen and retinal pigment epithelium (RPE) abnormalities, whereas OCT shows changes and alterations in the composition and structure of retinal tissues. OCT can also be used as a measurement indicator for retinal thickness and reflectivity, showing changes and alterations in the composition and structure of retinal tissues (Elsharkawy et al. 2021). Retinal thickness and reflectivity can also be used as biomarkers for AMD, where thickening or thinning of retinal layers can indicate disease progression, while the presence of focal hyperreflective RPE undulation is an indicator for the presence of drusen (Flores et al. 2021).

2.1 AMD prevalence and statistical analysis

Based on three large population-based studies, the Beaver Dam Eye Study (BDES) in the United States, the Blue Mountains Eye Study (BMES) in Australia, and the Rotterdam Study (RS) in the Netherlands, the prevalence of late AMD prediction was 0.2% for people between 55 and 64 years, expanding to 13.1% for people over 85 years old (Mitchell et al. 2018). According to BDES's ten years of follow-up (Klein et al. 2007), the prevalence of AMD in adults older than 43 years and younger than 54 years increased by an average of 4.2% and by 46.2% in those aged 75 and above.

The incidence of early and late AMD stages fluctuated depending on population, regional, and residential variables (Deng et al. 2022). According to Rein et al. (2022) using Bayesian meta-regression on the overall findings from the Centers for Disease Control and Prevention's (CDC) Vision and Eye Health Surveillance System (VRHSS), it was estimated that 12.6% of Americans aged 40 and older had AMD in 2019. It is estimated that the number of patients with AMD will increase to 196 million in 2020 and 288 million in 2040 (Wong et al. 2014), where Fig. 3 shows the predicted global prevalence in 2040 according to (Wong et al. 2014). As a chronic retinal disorder causing irreversible vision loss, no grade of AMD can be completely cured; however, early diagnosis allows for sooner medical intervention, which can help in preserving eyesight and slowing its progression (Wang et al. 2022).

The most significant risk factor is age, especially among Caucasians (National Institutes of Health 2021). Elderly Caucasians with a family history of AMD, who are also smokers, are advised to improve their lifestyle. This includes quitting smoking, engaging in regular exercise, adopting a healthy diet, undergoing routine eye examinations, and addressing other medical issues such as hypertension and hypercholesterolemia.

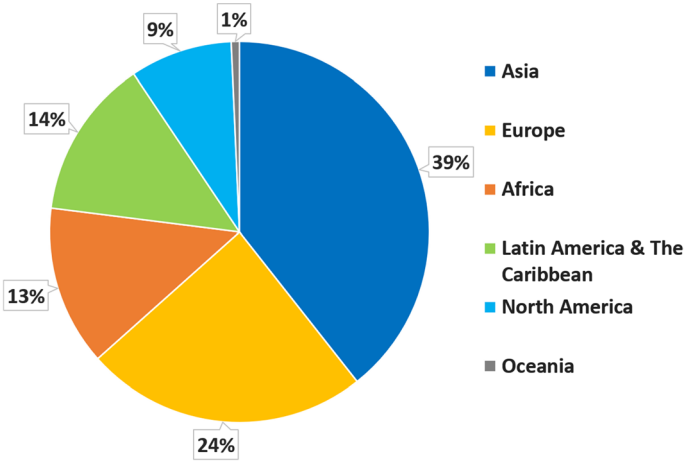

Fig. 3 The predicted global prevalence of AMD in 2040

2.2 Pathophysiology and grading

The exact pathophysiology involved in the development of AMD is unclear; however, it is known that the formation of drusen is a result of aging and environmental factors such as oxidative stress, chronic inflammation, and lipid deposition that result in changes to the extracellular environment (Fleckenstein et al. 2021). Drusen, presenting as focal extracellular deposits, can cause vision impairment. The size and number of these deposits can be used to characterize AMD and estimate the risk of disease progression (Thomas et al. 2021).

Dry AMD is classified into three grades: early, intermediate, and late dry AMD, also known as geographic atrophy (GA), where blind spots appear first in the parafoveal area, then consolidate and grow to include the foveal center, resulting in significant central vision loss (Fletcher et al. 2012). Dry AMD can develop into wet AMD at any point (Hobbs and Pierce 2022). Wet AMD is always considered a late stage, where visual loss may occur and develop rapidly. This occurs when choroidal neovascularization (CNV) develops underneath the macula (Elsharkawy et al. 2021). A patient diagnosed with wet AMD will be classified as having either active or inactive wet AMD. Inactive wet AMD has no leakage of blood or fluid behind the retina, but it requires periodic checks as it might become active again (Elsharkawy et al. 2021; Klein et al. 2002). Retinal angiomatous proliferation (RAP) is a subtype of wet AMD in which anastomosis forms between the choroidal and retinal vasculature, resulting in hyperfluorescence and hemorrhage as early and late hallmarks of the disease, respectively (Hobbs and Pierce 2022). Late presentation and diagnosis of RAP may be due to difficulty visualizing pathological changes and a complex clinical picture that is similar to other types of neovascularization such as polypoidal choroidal vasculopathy (PCV) (Ciardella et al. 2004; Dansingani et al. 2015; Polito et al. 2006). PCV pathophysiology is rooted in microaneurysms in the inner choroidal vessels, which can cause endothelial thinning and retinal epithelial detachment, resulting in visual symptoms such as metamorphopsia, central scotoma, and elevated orange-red lesions (Ciardella et al. 2004).

The hallmarks of AMD are the production of drusen, which are accumulations of proteins and lipids, and pigmentary abnormalities at the macula that are a predictor of

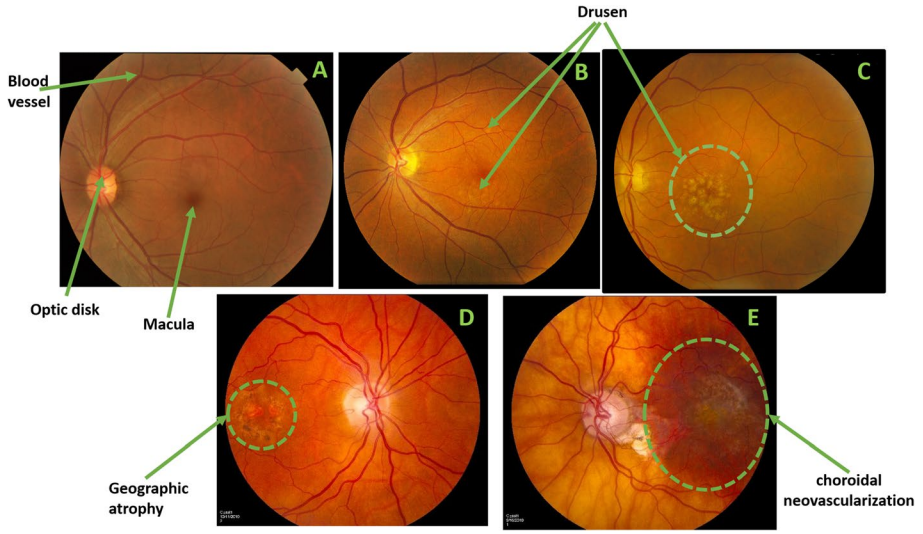

Fig. 4 Samples of retinal fundus image where **A** presents normal health retinal, **B** presents Early dry AMD grade where few small-sized drusen appear, **C** presents Intermediate dry AMD multiple intermediate-sized drusen and at least one large drusen appear, **D** presents Late dry AMD where there is evidence of GA, **E** presents Late Wet where CNV appears

Table 1 AREDS Classification of AMD

AMD grading	AREDS category	Characteristics (shown by Fundus images and OCT scans)
No AMD	1	Almost no or few (1–5) small drusen (< 63 µm in diameter)
Early AMD	2	Combination of multiple small drusen (< 63 µm in diameter) few intermediate drusen (63–125 µm) in diameter or mild RPE abnormalities
Intermediate AMD	3	Numerous intermediate drusen At least one large drusen (> 125 µm in diameter) Geographic atrophy: not involving center of fovea
Advanced AMD	4	Geographic atrophy involving fovea Neovascular maculopathy in the form of a CNV membrane or a disciform scar

the progression of AMD (Hernández-Zimbrón et al. 2018; Klein et al. 2002; Thomas et al. 2021). Changes in drusen size and density indicate a high risk of AMD development (Thomas et al. 2021) and grade progression (Ferris et al. 2005). AMD grades are classified according to the evidence of soft drusen, size of the drusen, and RPE abnormalities (Asia et al. 2022; Ferris III et al. 2013). Risk assessment and severity of AMD are primarily dependent on the patient's age, lifestyle factors such as smoking and nutrition, and family history of AMD (Al-Zamil and Yassin 2017; Ferris III et al. 2013). Figures 4 and 5 show different fundus and OCT images to differentiate between the normal retina and AMD-affected retina with different grades, respectively. Table 1 shows the characteristics

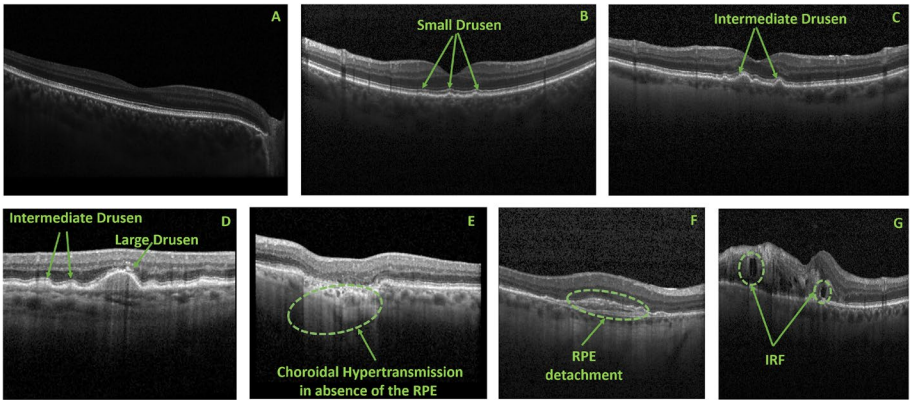

Fig. 5 Samples of retinal OCT images where **A** presents normal health retina, **B**, **C** present early dry AMD grade where few small-sized and intermediate-sized drusen appear, **D** presents intermediate dry AMD, where multiple intermediate-sized and one large-sized drusen appear; **E** presents late dry AMD, where there is choroidal hypertransmission under the area of absent RPE, **F** presents inactive wet AMD where RPE detachment occurred, and **G** presents active wet AMD showing the presence of intra-retinal fluid (IRF)

and grading of AMD according to the Age-Related Eye Disease Study (AREDS) (Al-Zamil and Yassin 2017; Dong et al. 2021; Ferris III et al. 2013; Hobbs and Pierce 2022; Keel et al. 2019).

2.3 Prevention and treatment

Strategies to prevent the development of AMD primarily target environmental risk factors. In addition to commonly recommended practices such as regular eye examinations, maintaining a balanced, healthy diet, and engaging in regular exercise, protecting the eyes from UV light-induced oxidative stress is a key measure for preventing AMD. Smoking cessation is highly advised, given that the likelihood of developing AMD is two to three times higher in smokers than in non-smokers (Thornton et al. 2005). Studies have supported the idea that the risk of early AMD can be decreased through dietary supplementation with nutrients such as beta-carotene, omega-3 fatty acids, and zinc (Di Carlo and Augustin 2021).

Treatment options for AMD are limited, with injectable therapies predominantly targeting neovascular signaling agents such as vascular endothelial growth factor (VEGF). These therapies were approved for use in wet AMD in 2006 and have been the mainstay in disease management (Maguire et al. 2016; Stahl 2020). However, the impact of anti-VEGF injections varies among patients, leading to reported differences in efficacy in the short and long term. Furthermore, central vision loss that results from irreversible photoreceptor atrophy does not respond to anti-VEGF injections (Fleckenstein et al. 2021).

2.4 Imaging modalities and diagnosis

Diagnosis of AMD requires medical imaging assessment using either CFP, SD-OCT scan, or fluorescein angiography (Gehrs et al. 2006; Lim et al. 2012). CFP involves capturing a high-resolution, color image of the retina, including the macula. Follow-up imaging can

assist in tracking disease progression; however, retinal changes seen in AMD, such as atrophy, may be difficult to identify on fundus imaging, and studies have attempted to automate detection with ML (Keenan et al. 2019).

SD-OCT differs from fundus photography in that it provides detailed cross-sectional images of the retina and its layers. SD-OCT measures reflections from low-coherence light that are reflected from the retina to create depth profiles of the macula (A-scans) (Le and Patel 2020). The cross-sectional view of the retina allows for numerous benefits in diagnosing and tracking AMD progression. The high-resolution scans contribute to the improved detection rates of AMD at an earlier stage, allowing for timely identification of retinal thickness, edema, and structural alterations (Regatieri et al. 2011).

Three-dimensional Fourier-domain OCT (3D-FD-OCT) can also be used in diagnosing and following patients with AMD; however, its use is not common in clinical practice(Menke et al. 2008). 3D-FD-OCT differs from SD-OCT in that it provides a higher number of acquired B-scans, yielding high-definition 3D images (Bouma et al. 2009). 3D-FD-OCT can provide isolated 3D images of certain retinal layers for visualization of the presence and extent of drusen, RPE detachment, and CNV.

CFP is widely used for retinal disease detection. It is available in clinical settings, faster, and lower in cost than OCT. CFP detects the retinal surface abnormality and visualizes retinal disease lesions, while OCT provides more detailed information, assessing the retinal thickness and giving more details about retinal morphology and layers. The limitations of CFP are due to its 2D image production, lack of visualization details (Saleh et al. 2022), and having lower sensitivity than OCT in identifying CNV of the lesion of wet AMD (Victor 2019). Meanwhile, OCT has limitations in grading CNV, therefore combining other imaging modalities with OCT.

2.5 AI approaches in AMD

Nowadays, developing healthcare-related AI applications to detect disease is encouraged due to the need for developing tools to assist doctors in the early diagnosis of diseases, as well as the availability of medical imaging technologies and the success records of using ML approaches architecture in developing powerful models. Applying AI approaches, particularly via computer vision (CV), affects ophthalmology and plays an important role in scientific research. Whereas AI-based CAD systems analyze medical images with high accuracy, assisting in diagnosing and detecting retinal disorders such as AMD through examining different medical imaging modalities such as CFP and OCT scans. These systems provide consistent, accurate outcomes, helping in the early diagnosis of the disease, detecting its severity level, and identifying its different biomarkers and lesions, enhancing the patient's everyday living conditions.

In ML, the machine learns how to imitate human behavior (Ongsulee 2017). Its approaches include Support Vector Machine (SVM) (Hearst et al. 1998) , K-nearest neighbor (k-NN) (Peterson 2009) , decision tree (DT) (Song and Ying 2015) , logistic regression (LR), and Naive Bayes (NB) (Rish et al. 2001) methods. ML approaches have shown promising outcomes, nevertheless, they have time-consuming constraints due to extracting features that require identifying and selecting meaningful features from data manually. Meanwhile, DL, a subset of ML, uses a deep neural network composed of multiple layers of interconnected neurons, inspired by the basic functionality of human brain neurons. DL models learn from large datasets where the training phase adjusts the weights of interconnection between neurons, after which the trained model can make its own

decisions without human intervention. DL approaches include CNN, recurrent neural networks (RNN) (Salehinejad et al. 2017) , TL techniques, generative adversarial networks (GANs) (Creswell et al. 2018), vision transformers (ViTs) (Dosovitskiy et al. 2020), and autoencoders (AE) (Bank et al. 2020). AE are versatile tools in data processing tasks. They extract informative features and filter out noise by converting input data into minimal distortion outputs. They compress and reconstruct the input data through three stages: an encoder that compresses the input's dimensional representation, a latent space that handles the dimensionality reduction, and a decoder that reconstructs the original data. AE are useful for data compression, image-to-image translation, denoising, and anomaly detection. Although AE are useful for compression and dimensionality reduction challenges, we risk losing fine feature details and information; therefore, it requires careful tuning to avoid overfitting.

With the ability to generate synthetic images, GAN can help augment datasets and improve model robustness by generating synthetic retinal images, hence overcoming the limitation of the available dataset samples. Meanwhile, ViTs are DL models that use self-attention mechanisms inspired by transformer models developed to solve natural language processing (NLP) challenges, offer scalability to larger input sizes, and offer flexibility in handling diverse input modalities. In CV, the image dataset is input to a multi-layer transformer encoder model, which includes self-attention layers and feedforward neural network layers, where the input image is divided into fixed-size patches and treated as sequences.

These techniques are powerful and effective approaches for detecting and diagnosing retinal disorders. However, each has its limitations. AI requires high processing costs. DL and ViTs require large datasets to perform efficiently with high precision; however, we can overcome this constraint by utilizing GAN. (Oliveira et al. 2024) proposed StyleGAN2 model to generate synthetic fundus images with and without AMD using CFP from iChallenge-AMD, ODIR-2019, and RIADD public datasets recording Fréchet inception distance (FID) of 166.17. It should be considered that the generated images may not correspond to real-world images, even unintentionally.

Generally, CAD systems with AI-based approaches are useful for automatic data analysis, segmentation, retinal disorder detection, and severity level classification. Researchers anticipate developing systems to diagnose AMD, predict its progression, and suggest customized prescriptions.

2.6 AMD datasets

Datasets are essential for training, validating, and testing models. Datasets are either public or private (local) datasets, each with limitations and benefits that impact research outcomes depending on the size of the data and its availability. Public datasets are accessible and may be large enough for training a model. However, samples may be of low quality and represent multiple diseases. Private datasets are accessibility restricted and tailored to specific disease research. Both types of datasets may be geographically biased and lack population diversity. Their size limitation may require applying different techniques, such as data augmentation, to increase dataset size artificially.

This review encompasses studies focused on diagnosing and grading AMD using publicly available datasets for fundus photography and OCT scans, as listed in Table 2, including iChallenge-AMD , ARIA , AREDS AREDS1 (2006), STARE , and OCT-based datasets such as Duke (Srinivasan et al. 2014), Mendeley (Hassan et al. 2019), NOOR , and OCTID (Gholami et al. 2020).

Table 2 Available public datasets for fundus and OCT images used for AMD analysis

Imaging type	Clinical dataset	Number of images	Resource link
Fundus	iChallenge-AMD	1200	https://tinyurl.com/iChallengePubDS
	AREDS AREDS1 , AREDS2 (Clemons et al. 2003)	72K	https://tinyurl.com/aredsPubDS
	STARE (STARE)	400	https://tinyurl.com/starePubDS
OCT	Duke (Srinivasan et al. 2014)	1407 Normal, 723 AMD	https://tinyurl.com/dukePubDS
	Mendeley (Hassan et al. 2019)	84K	https://tinyurl.com/mendelyPubDS
	OCTID (Gholami et al. 2020)	206 Normal, 55 AMD	https://tinyurl.com/octidPubDS
	NOOR (Rasti et al. 2017)	50 Normal, 48 AMD, 50 DME	https://tinyurl.com/noorPubDS

3 AMD detection and classification approaches

Early detection of AMD can help prevent its progression; however, dry AMD may become wet AMD without any indications (Hobbs and Pierce 2022). In the literature, several studies have tried to classify and discriminate between AMD's different grades and normal retinas (Al-Zamil and Yassin 2017; Dong et al. 2021; Ferris III et al. 2013; Hobbs and Pierce 2022; Keel et al. 2019;). Different automated approaches have been researched and developed to identify and classify different gradings of AMD from various medical imaging checks, adopting diverse ML, DL, and TL techniques.

A clinical examination conducted by a healthcare professional marks the first step in identifying an illness. This examination involves a thorough analysis of the patient's medical history, symptoms, and signs, in addition to performing different imaging modalities to establish a diagnosis. Timely detection of an illness is crucial, allowing for prompt treatment and effective management, thereby mitigating its progression and potential consequences. ML and AI-based techniques to identify diseases have shown potential and promising approaches. By evaluating massive patient information and medical records databases, AI systems may detect patterns and signals that humans may overlook.

(Peng et al. 2019) developed the DeepSeeNet DL model and used a dataset consisting of 58,402 fundus images for training and testing on 900 fundus images from AREDS. The model recorded better performance compared to human retinal specialists for detecting AMD and differentiating between its grades, as it recorded an accuracy of 67.1%. In contrast, human retinal specialists recorded an accuracy of 59.9%.

(Burlina et al. 2017) used TL with a linear support vector machine (LSVM) (Tang 2013) classifier and compared the performance between computer and physician grading using the NIH AREDS dataset consisting of 5664 fundus images. Performing the 4-Class classification experiment to detect whether it is no AMD, early AMD, intermediate AMD, or advanced AMD recorded an accuracy of 79.4%, whereas physician grading recorded an accuracy of 75.8% while the 3-Class classification experiment to discriminate between no or early AMD, intermediate AMD, or advanced AMD recorded an accuracy of 81.5%, whereas physician grading recorded an accuracy of 85.0%. On the other hand, the binary

classification experiment recorded an accuracy of 93.4%, whereas physician grading recorded an accuracy of 95.2%.

3.1 AMD detection using OCT scans

Table 3 shows several studies that implemented the binary classification for AMD detection according to the presence of different biomarkers using OCT scans. Ogundokun et al. (2023) implemented Inception-V3 (Szegedy et al. 2015) and applied data augmentation to avoid any problem related to using imbalanced OCT dataset scans, recording an overall accuracy of 96.41%, precision of 94.24%, AUC of 0.9633, and specificity of 94.82%. Wang et al. (2023) proposed an improved VGG16 (Simonyan and Zisserman 2014). The model recorded an accuracy of 96.62%, a sensitivity of 96%, a specificity of 96%, and an AUC of 0.9458 using 32k OCT scans for testing and training the model. He et al. (2022) proposed a TL-CNN based on ResNet50 (He et al. 2016) and local outlier factor (LOF) algorithm for classification training the model on OCT scans, recording accuracy of 99.87%, and AUC of 1.00 using the UCSD dataset and accuracy of 97.56% and an AUC of 0.9954 using the Duke dataset. An et al. (2019) proposed two stages for classification using the VGG16 pretrained model. The first stage recorded an accuracy of 99.2% and an AUC of 0.999, while the second stage recorded an accuracy of 95.1% and an AUC of 0.992, where a private dataset of 1625 OCT scans was used. The first stage performed a binary classification of whether AMD was detected or not, while the second stage succeeded in classifying AMD into AMD with fluid or AMD without fluid. Thomas et al. (2021) implemented a CNN composed of 7-layers. The model recorded accuracy ranging from 96.66% to 99.73% using four different OCT datasets for training and testing scans, with OCT scans from the Mendeley dataset used for training and OCT scans from the OCTID, Noor, and Duke datasets used for testing. Hwang et al. (2021) performed a binary classification to differentiate between RAP and PCV, proposing a novel model for detecting neovascular AMD (nAMD) and distinguishing between retinal RAP and PCV. The model recorded an accuracy of 89.1%, a sensitivity of 89.4%, and a specificity of 88.8% compared to VGG16, ResNet50, and Inception-V3 using a private dataset from Hangil Eye Hospital consisting of OCT scans for normal retina, RAP, and PCV. Wang et al. (2020) proposed a model combining Mel Frequency Cepstral Coefficient (MFCC) and Haralick texture features with a random forest classifier, recording an overall accuracy of 70.11% using a dataset consisting of 437 OCT scans from Northwestern Memorial Hospital. Lee et al. (2017) proposed a modified version of the VGG16 model. The proposed model recorded an accuracy of 87.63%, and an ROC of 92.78%, using a dataset composed of 101,002 OCT scans. Sahoo et al. (2023) proposed weighted majority voting (WMV) that evaluates the weight of four different classifiers based on SVM, k-NN, DT, and LR to differentiate between dry AMD and normal OCT scans. The model was trained using the OCTID, recording an accuracy of 96.15%, a sensitivity of 95.45%, a specificity of 96.43%, a precision of 91.3%, and an AUC of 0.985. The proposed model used the Noor dataset for testing and recorded an accuracy of 96.94%, a sensitivity of 97.87%, a specificity of 96.08%, a precision of 95.83%, and an AUC of 0.988. Although WMV improves performance by combining different models, it may confront limitations due to the complexity of implementation difficulties, and sensitivity to inadequate models that lead to overfitting risk. Motozawa et al. (2019) succeeded in detecting AMD and differentiating between exudative AMD and non-exudative AMD by proposing two models for classification using 20k OCT images from the Doheny Eye Centers, a private dataset composed of 1621 OCT scans. The first model is a CNN, and the second

Table 3 Modern research and developments for detecting AMD using OCT medical imaging modalities

Methodology and references	Dataset (#images)	Performance measurement	Classification	Advantage	Limitation
ResNet50 (Chen et al. 2023)	Fujian Provincial Hospital (37K)	Acc.: 98.5% Sens.: 98.7% Spec.: 98.4% F1-score: 97.7%	Normal or abnormal	Reusable pre-trained model,improve generalization ability	Architecture complexity time consumption large number of parameter insuffiecent samples
Inception-V3 (Ogundokun et al. 2023)	OCIR (5748)	Acc.: 96.41% Prec.: 94.24% Spec.: 94.82% AUC: 0.9633	AMD or not	Reusable pre-trained model, overcome data samples limitation, attempt to boarden classification challenges	High computational cost, large number of parameters, overfitting risk
Improved VGG16 (Wang et al. 2023)	Private (32K)	Acc.: 96.62% Sens.: 96% AUC: 0.9458	AMD or not	Reuse pre-trained model, powerful provide explanation for model decision,	High data quality high time consumption
semi-sequential classifiers (Zang et al. 2023)	Private (562)	Acc.: 94.53% Spec.: 96.88% Sens.: 88.28% AUC: 0.95	AMD or not	Performed multiple classification in parallel to detect retinal disorder	Biased to local dataset, require large dataset, high computational cost, and overfitting risk
WMV (Sahoo et al. 2023)	Training: NOOR	Acc.: 96.94% Sens.: 97.87% Spec.: 96.08% Prec.: 95.83% AUC: 0.988	Dry AMD or normal	Combine different models to improve performance useful for fast eye-screening for early detection of dry AMD	High computational cost, architecture complexity, sensitive to poor model
	Testing: OCTID	Acc.: 96.15% Sens.: 95.45% Spec.:96.43% Prec.: 91.3% AUC: 0.985			

Table 3 (continued)

Methodology and references	Dataset (#images)	Performance measurement	Classification	Advantage	Limitation
ResNet with attention (Wongchaisuwat et al. 2022)	Private (3505)	Acc.: 83% Spec.: 79% Sens.: 69% F1-score: 76% AUC.: 0.81	wet AMD or PCV	Good attempt to differentiate between PCV and wet AMD applying TL technique to overcome data limitation	Endure biased, and insufficient data, overfitting risk
VGG16 (Kadry et al. 2022)	Private (200)	Acc.: 97.5% Spec.: 97.92% Sens.: 97.08% Prec.: 97.89%	AMD or not	Shows that OCT outperforms CFP, using TF technique to overcome limited dataset size	Require high data quality, high time consumption, biased to local dataset, overfitting risk
ResNet50 and LOF (He et al. 2022)	UCSD	Acc.: 99.87% AUC: 1.0	AMD or not	No preprocessing needed, worthy attempt to diagnose AMD	Complex architecture, high time consumption, large parameter number
	Duke	Acc.: 97.56% AUC: 0.9954			
DCNN (Hwang et al. 2021)	Private (3951)	Acc.: 89.1% Spec.: 88.80% Sens.: 89.4%	RAP or PCV	Good performance indicator to differentiate between RAP and PCV	Imbalanced dataset, overfitting risk biased to local dataset
7-layers CNN (Thomas et al. 2021)	Training: Mendely OCTID	Acc.: 99.73% AUC: 0.9999	AMD or not	Worthy attempt to diagnose AMD, less number of parameters, reduced system complexity	Inadequate to differentiate between AMD grades.
	Testing: NOOR Duke	Acc.: 96.66% AUC: 1.0			
Combine MFCC and HTF with RF classifier (Wang et al. 2020)	Private (438)	Acc.: 70.11% Sens.: 68.58% Spec.: 75.40%	AMD or not	Good attempt for generalization capability, manually extracting features guarantees extracting the most significant and impactful features	Endure biased and insufficient data, imbalanced dataset, overfitting risk

Table 3 (continued)

Methodology and references	Dataset (#images)	Performance measurement	Classification	Advantage	Limitation
Two stages of VGG16 (An et al. 2019)	Private (1625)	First stage: Acc.: 99.2% AUC: 0.999	AMD or not	Using TF technique to overcome limited dataset size	Complex architecture, biased to local dataset, require high image quality overfitting risk
		Second stage: Acc.: 95.1% AUC: 0.992	AMD with or without fluid		
CNN (Motozawa et al. 2019)	Private (1621)	Acc.: 93.9% Spec.: 88.3% Sens.: 98.4%	Having exudative or not	Applied TF technique using their CNN to overcome dataset limitation	Biased to local dataset, require high image quality, overfitting risk
Modified VGG16 (Lee et al. 2017)	Private (101k)	Acc.: 87.63% ROC: 92.78%	AMD or not	Using TF technique to overcome limited dataset size	Biased to local dataset, require high image quality, complex architecture

model performed a TL-CNN based on using their already constructed pre-trained CNN model, recording an accuracy of 93.9%, a sensitivity of 98.4%, and a specificity of 88.3%. Zang et al. (2023) proposed a DL framework composed of semi-sequential classifiers to perform multiple binary classifications among AMD, DR, and glaucoma to differentiate between the normal retina and the presence or absence of the respective diseases, recording accuracy of 94.53%, a sensitivity of 88.28%, a specificity of 96.88%, and an AUC of 0.95 for detecting AMD and accuracy of 90.19%, a sensitivity of 90%, a specificity of 90.27%, and an AUC of 0.91 for detecting DR, using a dataset composed of 526 OCT images. Chen et al. (2021) proposed a TL-CNN based on using different pre-trained models to perform binary classification to differentiate between AMD and diabetic macular edema (DME), where VGG19, ResNet101, and ResNet50 recorded the highest accuracy rates of 99.42%, 99.19%, and 99.09%, respectively. Additionally, for multi-class classification to differentiate between OCT scans of no-AMD grade, CNV, Drusen, and DME, both models recorded accuracy rates of 99.48%, 99.28%, and 99.28% respectively. Chen et al. (2023) proposed a TL-CNN based on using the ResNet50 pre-trained model to detect normal and abnormal OCT scans from a dataset consisting of 37,138 images gathered from Fujian Provincial Hospital, recording accuracy of 98.5%, a sensitivity of 98.7%, a specificity of 98.4%, and an F1-score of 97.7%. Although using YOLO-V3 (Redmon and Farhadi 2018) struggles to identify small objects, the model performed multi-class multi-label classification and succeeded in detecting 10 different retinal lesions, predicting and differentiating between AMD lesions and vitreomacular traction syndrome (VMT), and recorded an overall accuracy of 99%, sensitivity of 98%, specificity of 98% and f1-score of 97%. For VMT prediction, the model recorded an accuracy of 99.3%, a specificity of 99.5%, a sensitivity of 98.4%, and an F1-score of 98.4%. For AMD detection, the model recorded an accuracy of 99.5%, a specificity of 98.3%, a sensitivity of 98.3%, and an F1-score of 97.9%.

3.2 AMD detection using Fundus photography

Table 4 shows several studies that implemented the binary classification for AMD detection according to the presence of different biomarkers using fundus photography. Chakraborty and Pramanik (2022) implemented DCNN composed of 13 layers and applied data augmentation using the iChallenge-AMD dataset. The model recorded an accuracy of 89.75% without data augmentation, whereas it recorded 91.69% with 4-time data augmentation and 99.45% with 16-time data augmentation. When using the ARIA dataset, the model recorded an accuracy of 90% without data augmentation, 93.03% with 4-time data augmentation, and 99.55% with 16-time data augmentation. Pečiulis et al. (2021) proposed a TL-CNN based for detecting AMD according to segmenting its lesion zone using different pre-trained models: ResNet50, ResNet101, UNet, and MobileNetV3 (Howard et al. 2019), which recorded the best accuracy of 93.55% using a dataset from the Lithuanian University of Health Sciences Department of Ophthalmology. Keel et al. (2019) developed a DL algorithm for detecting AMD using a dataset consisting of 56,113 fundus images collected from the Chinese population, recording an AUC of 0.995, a sensitivity of 96.7%, and a specificity of 96.4%. Tan et al. (2018) implemented a DCNN composed of 14 layers and used data augmentation to avoid overfitting. The proposed model recorded an accuracy of 91.17%, sensitivity of 92.66%, and specificity of 88.56% by applying blindfold and an accuracy of 95.45%, sensitivity of 96.43%, and specificity of 93.75% when applying ten-fold cross-validation strategies using a dataset composed of 402 normal and 708 AMD fundus images. Burlina et al. (2017) proposed two DCNN implementations; the

Table 4 Modern research and developments for detecting AMD using Fundus medical imaging modalities

Methodology and references	Dataset (#images)	Performance measurement	Classification	Advantage	Limitation
ResNet18 (Oliveira et al. 2024)	synthetic CFP (6k)	Acc.: 85% Spec.:80% Sens.:90%	AMD or not	Using of GANs overcome the local dataset limitation	Synthetic images that may not correspond to reality.
13-layers DCNN (Chakraborty and Pramanik 2022)	ARIA	Acc.: 99.55% Sens.: 98.55% Spec.: 100% Prec.: 100% F1-score: 99.26%	AMD or not	No need for extracting features manually good performance indicator	Required large dataset, overfitting risk inadequate to differentiate between AMD grades
	iChallenge-AMD	Acc.: 99.45% Sens.: 98.22% Spec.: 99.82% Prec.: 99.35% F1-score: 98.77%	AMD or not		
VGG16 (Kadry et al. 2022)	Private (400)	Acc.: 97.08% Spec.: 97.5% Sens.: 96.6% Prec.: 97.479%	AMD or not	Shows that OCT outperforms CFP, using TF technique to overcome limited dataset size	Biased to local database, overfitting risk, high consuming time, require high data quality
ResNet50 (Takhchidi et al. 2021)	Private (1200)	Acc.: 96.6% Spec.: 94.3% Sens.: 99%	AMD or not	Using TF technique to overcome limited dataset size,	Fine-tuning, overfitting risk biased to local dataset
MobileNetV3 (Pečiulis et al. 2021)	Private	Acc.: 99.93% Sens.: 99.87% Spec.: 99.99%	AMD lesion or not	Using TF technique to overcome limited dataset size, good attempt for generalization capability	Limited dataset, required data preprocessing, overfitting risk fine-tuning
DCNN (Bhuiyan et al. 2020)	AREDS	Acc.: 99.2% Sens.: 98.9% Spec.: 99.5%	(normal/early) or (intermediate/late)	High performance indicator	Required high image quality, biased to local dataset
CNN (Zapata et al. 2020)	Optretina (306k)	Acc.:86.3% AUC: 0.936	AMD or not	No need for extracting features manually	Required high image quality

Table 4 (continued)

Methodology and references	Dataset (#images)	Performance measurement	Classification	Advantage	Limitation
DCNN (Keel et al. 2019)	Private (30k)	Spec.: 96.4% Sens.: 96.7% AUC: 0.995	AMD or not	No need for extracting features manually	Required high image quality high time consumption, imbalanced dataset
14-layers DCNN (Tan et al. 2018)	Private (1110)	Blindfold Acc.: 91.17% Sens.: 92.66% Spec.: 88.56% Ten-fold Acc.: 95.45% Sens.: 96.43% Spec.: 93.75%	AMD or not	Fully automated model, no need for extracting features manually or a classifier	Biased to local dataset, overfitting risk, required high image quality
DCNN-A (Burlina et al. 2017)	AREDS	Acc.: 91.6% Sens.: 88.4% Spec.: 94.1 kappa: 0.829	AMD or not	Good attempt to diagnose AMD	Imbalanced dataset, required high image quality, biased to dataset
LSVM (Burlina et al. 2017)	AREDS	Acc.: 93.4% kappa: 0.8482	AMD or not	Using TF technique to overcome dataset limitation, the model closed to physician good attempt to diagnose AMD	Required high image quality and, fine-tuning, imbalanced dataset

first DCNN-A method used the AlexNet model, and the second DCNN-U method used the OverFeat DCNN model. Using 13,000 fundus images from the National Institutes of Health (NIH) AREDS dataset, the proposed model recorded accuracy of 91.6% and 83.7% for the DCNN-A and DCNN-U models, respectively. Pham et al. (2022) proposed a GAN-based model called Multi-Modal GAN (MuMo-GAN), capable of generating synthetic fundus images of detecting drusen changes over time. The proposed model cannot monitor the progression from early to late AMD. MuMo-GAN employs a generator with 6 ResNet blocks, and the discriminator is implemented using PatchGAN, recording the best accuracy and the best FID scores of 55% and 69.6, respectively, in comparison to PAN and Pix2Pix models, using a dataset composed of 8196 fundus images.

3.3 AMD grading and classification using OCT scans

Table 5 shows several studies that implemented the multi-class classification for different gradings of AMD using OCT scans. Yan et al. (2021) proposed ResNet34 integrated with convolutional block attention (CBAM) for detecting the CNV activity and distinguishing between a normal retina, drusen, active wet AMD, and inactive wet AMD recording precision of 93.7%, 84.3%, 81.2%, and 97.7% for normal retina, drusen, active wet AMD, and inactive wet, respectively, sensitivity of 96.5%, 87.3%, 80%, and 90.2% for normal retina, drusen, active wet AMD and inactive wet, respectively, and AUC of 0.9925, 0.9395, 0.9476, and 0.9880 for normal retina, drusen, active wet AMD, and inactive wet, respectively. The system of Elsharkawy et al. (2024) is capable of differentiating between a normal retina, AMD grades (early, intermediate, GA, inactive wet, and active wet), and non-AMD retinal disorder. They recorded an overall accuracy of 90.82% and a kappa score of 0.891, proposing an explainable artificial intelligence (xAI) system using the DeepLabV3+ network with the ResNet50 model, using a private OCT dataset composed of 1285 images. Their proposed model recorded sensitivity of 93.5%, 83.33%, 92.04%, 92.04%, 90.47%, 91.35%, 91.11%, and 90.4% for normal retina, early AMD, intermediate AMD, GA, inactive wet AMD, active wet AMD, and non-AMD retinal diseases, respectively, and recorded precision of 91.13%, 80.45%, 94.18%, 86.36%, 88.09%, 91.11%, and 95.76% for normal retina, early AMD, intermediate AMD, GA, inactive wet AMD, active wet AMD, and non-AMD retinal diseases, respectively. The limitation of this study is that recording precision and sensitivity are lower than 84% for early AMD and intermediate AMD, respectively. Saha et al. (2019) proposed a TL-CNN based on using different pre-trained models, Inception-V3, ResNet50, and Inception-ResNet50, to detect and classify early AMD biomarkers such as intraretinal hyperreflective foci (IHRF), hyporeflective foci (hRF) within drusenoid lesion, and subretinal drusenoid deposit (SDD), where Inception-ResNet50 recorded good performance for detecting the presence of IHRF, hRF, and SDD, recording accuracy of 89%, 88%, and 86%, respectively, using 20k OCT images from the Doheny Eye Centers. Azizi et al. (2024) used pre-trained medical vision transformer (MedViT) model to differentiate between a normal retina, drusen, and CNV using UCSD and NEH public datasets. They used stitchable neural networks to select an ideal MedViT model from two MedViT family models (micro and tiny MedViT). Both recorded similar findings: micro MedViT recorded an accuracy, specificity, and sensitivity of 97.7%, 98.9%, and 97.5%, respectively, using 12k samples of the NEH dataset, and recorded an accuracy, specificity, and sensitivity of 82.8%, 92.8%, and 80.8% respectively, using 96k samples of UCSD dataset. Sotoudeh-Paima et al. (2022) proposed a multi-scale CNN based on the Feature Pyramid Network (FPN) combined with pre-trained models VGG16, ResNet50, DenseNet121, and

Table 5 Modern research and developments for detecting and identifying AMD grading utilizing OCT medical imaging modalities

Methodology and Reference	Dataset (#images)	Performance measurement	Classification	Advantage	Limitation
MedViT (Azizi et al. 2024)	NEH (12k)	Acc.: 97.7% Spec.: 98.9% Sens.: 97.5%	Normal, drusen, and CNV (3-class)	Stitching overcome the need of large dataset, good performance indicator	Required high image quality, biased to dataset with class and pixel-wise labels
	UCSD (96K)	Acc.: 82.8% Spec.: 92.8% Sens.: 80.8%			
CNN (Gueddena et al. 2024)	private (934)	Overall metrics: Acc.: 99.6% Sens.: 97.6% Prec.: 97.6% F1-score: 97.6%	Normal, AMD, and DME (3-class)	High performance indicator, good attempt for generalization capability	Biased to dataset, overfitting risk, high image quality, imbalanced dataset
	DUKE (3212)	Overall metrics: Acc.: 99.53% Sens.: 99.66% Prec.: 99.66% F1-score: 99.66%			
Mobile-ViT (Akça et al. 2024)	Mendely (34k)	Overall metrics: Acc.: 99.17% Sens.: 99.59% Prec.: 99.59% F1-score: 99.89%	Normal, CNV, drusen, and DME (4-class)	Highest performance indicator compared to T2T-ViT and ViT	High image quality
xAI system using DeepLabV3+ network with ResNet50 (Elsharkawy et al. 2024)	Private (1285)	overall Acc.: 90.82% kappa: 0.84	Normal, early, intermediate, GA, active wet, inactive wet and non-AMD disease (7-class)	Classifyied wet AMD into active AMD and inactive AMD	inadequate to differentiate between early AMD and intermediate AMD

Table 5 (continued)

Methodology and Reference	Dataset (#images)	Performance measurement	Classification	Advantage	Limitation
CapsNet (Celebi et al. 2023)	Kaggle with Private (726)	Acc.: 98.07% Sens.: 96.72% Spec.: 99.98% F1-score: 98.03% AUC: 0.9869	Normal, dry, wet, and drusen (4-class)	Good attempt to detect different grads of AMD, high performance indicator	Imbalanced dataset required high image quality overfitting risk
CNN (Diao et al. 2023)	UCSD	Overall metrics: Acc.: 96.93% Sens.: 96.3% Spec.: 98.46% AUC: 0.995 kappa: 0.9540	Normal, CNV, and drusen (3-class)	Good performance indicator for discriminating between normal retina, drusen, and CNV	Required high image quality biased to dataset
Two ResNet stages (Leingang et al. 2023)	Private (3765)	Acc.: 88.3% Sens.: 83.5% Spec.: 89.9% F1-score: 83.1% AUC: 0.944	Normal, intermediate, GA, and nAMD (4-class)	Using TF technique to overcome limited dataset size, good attempt for generalization capability two stages guarantee effficient analysis	Complex architecture biased to dataset required high image quality overfitting risk
YOLO-V3 (Chen et al. 2023)	Fujian Provincial Hospital (37k)	Acc.: 99% Spec.: 98% Sens.: 98% F1-score: 97%	VMT syndrome, and AMD lesions (Multi-class Multi-lable)	High performance indicator for differentiating between AMD lesions, and VMT syndrome, worthy attempt for generalization capability, save time and resources	Biased to dataset required high image quality overfitting risk confront difficulty identifying small object

Table 5 (continued)

Methodology and Reference	Dataset (#images)	Performance measurement	Classification	Advantage	Limitation
VGG16 (Han et al. 2022)	Private (4749)	Overall metrics: Acc.: 87.4% Sens.: 83.25% Prec.: 84% F1-score: 83%	Normal, PCV, RAP, and typical AMD (4-class)	Using TF technique overcome dataset limitation, good attempt to distinguish between normal, and nAMD subtypes PCV, RAP and typical AMD	High computational cost, biased to dataset, large number of parameters overfitting risk
FPN integrated with VGG16 (Sotoudeh-Paima et al. 2022)	UCSD	Acc.: 92% Spec.: 95.8% Sens.: 91.80%	Normal, drusen, wet AMD, and DME (4-class)	Good performance indicator, use multi-scale receptive fields enabling varying OCT scales	High computational cost, complex architecture large number of parameters, require high image quality
	NEH	Acc.: 98.4% Spec.: 97.4% Sens.: 100%	Normal, drusen, CNV (3-class)		
ResNet34 integrated with convolutional block attention module (CBAM) (Yan et al. 2021)	Private and UCSD (65k)	Overall metrics: Sens.: 88.5% Prec.: 89.22% AUC: 0.9669	Normal, drusen, inactive wet AMD, and active wet AMD (4-class)	Novel model capable of differentiating between active and inactive wet AMD good performance indicator	Small private dataset required high image quality, biased to dataset fine-tuning
VGG19 (Chen et al. 2021)	Mendeley	Acc.: 99.48% Sens.: 99.48% Spec.: 99.83% Prec.: 99.49% F1-score: 99.48%	Normal, CNV, drusen and DME (4-class)	High performance indicator good attempt to distinguish between normal, CNV, DME, and drusen	High computational cost, complex architecture large number of parameters fine-tuning
Atten-ResNet (Li and Quan 2020)	Mendeley	Acc.: 95.7% Prec.: 95.2%	CNV, DME, Drusen, and normal (4-class)	Good performance indicator using attention mechanism to guide CNN in classification decision	Complex architecture high computational time

Table 5 (continued)

Methodology and Reference	Dataset (#images)	Performance measurement	Classification	Advantage	Limitation
VGG19 (Wang et al. 2020)	Private (498)	Overall metrics: Acc.: 93.14% Sens.: 93.99% Prec.: 94.08%	Wet, GA, drusen and normal (4-class)	Using TF technique overcome dataset limitation, high performance indicator good attempt to distinguish between normal, GA, wet, and drusen	Limited dataset complex architecture small dataset overfitting risk fine-tuning
ResNet18 (Serener and Serte 2019)	Mendeley (84k)	Acc.: 98.8% Sens.: 95.6% Spec.: 99.9% AUC: 0.93	Dry, wet DME, and normal (4-class)	Good performance indicator, using of ResNet18 outperform AlexNet	High computational cost, require high image quality, imbalanced dataset, overfitting risk
Inception- ResNet50 (Saha et al. 2019)	Doheny Eye Centers (20k)	Overall metrics: Acc.: 87% Sens.: 80% Spec.: 94% AUC: 0.87	Early AMD biomarkers IHRF, hRF, SSD (3-class)	Good attempt to broaden biomarkers identification challenges	High computational cost, large number of parameters require high image quality

EfficientNet-B0. When VGG16 was combined with FPN, the model recorded the best performance with an accuracy of 92%, a specificity of 95.8%, and a sensitivity of 91.8%, using OCT images from Noor Eye Hospital (NEH) for performing a 3-class classification to differentiate between normal, drusen, and CNV. When tested on the UCSD dataset, the model recorded an accuracy of 98.4%, a specificity of 97.4%, and a sensitivity of 100% for performing a 4-class classification to differentiate between a normal retina, drusen, AMD, and DME. Leingang et al. (2023) used ResNet18 integrated with ResNet34 for detecting and differentiate between normal retinal and AMD grades (intermediate, GA, nAMD) according to the presence of the biomarkers; macular atrophy (MA), and macular neovascularization (MNV), drusen recording accuracy of 88.3%, sensitivity of 83.5%, specificity of 89.9%, F1-score of 83.1%, and AUC: 0.944. Their proposed model is biased toward OCT images produced from the Topcon OCT scanner. Gueddena et al. (2024) propose a custom CNN model for differentiating between normal retina, DME, and AMD, recording an accuracy of 99.6% using a Tunisian private dataset composed of 934 OCT images and the public DUKE dataset. Their proposed model recorded better accuracy than InceptionV3, VGG16, and VGG19. Han et al. (2022) proposed 3 different TL-CNN pre-trained models: VGG16, VGG19, and ResNet. VGG16 recorded the best accuracy of 87.4% using a private dataset composed of 4749 OCT images to differentiate between normal retina and different grades of nAMD (PCV, RAP, and typical AMD). Akça et al. (2024) proposed three different ViT-based models to differentiate between normal retina, drusen, CNV, and DME using a 34k OCT image from the Mendely dataset, where Mobile-ViT recorded the highest accuracy of 99.17%, while Tokens-To-Token Vision Transformer (T2T-ViT) and ViT recorded accuracy of 96.07% and 95.14%, respectively. Li and Quan (2020) proposed an attention mechanism for a deep residual network (Atten-ResNet), an attention-based deep ResNet50. This was compared to applying a TL-CNN based on 3 different pre-trained models: VGG16, ResNet50, and a multi-scale oriented gradient histogram using a support vector machine (HOG-SVM). The model succeeded in differentiating between CNV, DME, Drusen, and normal retina, recording an overall accuracy of 95.7%, and a precision of 95.2%, using the Mendeley dataset. Wang et al. (2020) proposed a TL-CNN based on using a VGG19 pre-trained model to differentiate between wet AMD, GA, drusen, and normal OCT scans. They used a dataset collected from Northwestern Memorial Hospital composed of 396 OCT images for the training set and 102 images for the testing set, recording an overall accuracy of 93.14%. Serener and Serte (2019) proposed a TL-CNN based on using different pre-trained models, AlexNet and ResNet18, to differentiate between dry AMD, wet AMD, DME, and normal OCT scans. ResNet18 recorded the highest accuracy rates of 99.5% and 98.8% for detecting dry AMD and wet AMD, respectively, using the Mendely dataset.

3.4 AMD grading and classification using Fundus photography

Bhuiyan et al. (2020) implemented a DL model to perform binary classification, recording an accuracy of 99.2%, sensitivity of 98.9%, and specificity of 99.5% distinguishing between (normal/early) and (intermediate/late). They also performed a 4-class classification to differentiate between normal, early, intermediate, and advanced AMD, recording an accuracy of 96.1%. The model was also used for disease prediction, recording accuracy rates of 66.79% and 68.15% for predicting dry and wet AMD, respectively, for one-year progression. For two-year progression, the model recorded accuracy rates of 66.88% and 67.15%, respectively, using 116K CFP from AREDS for training and the Nutritional

AMD Treatment-2 (NAT-2) study for validation. Table 6 shows several studies that implemented the multi-class classification for different gradings of AMD using CFP. Ali et al. (2024) proposed AMDNet23 to diagnose three different retinal disorders and differentiate between normal retinal, AMD, cataract, and DR, recording an accuracy of 96.50%, specificity of 99.32%, sensitivity of 96.5%, precision of 96.51%, and F1-score of 96.49%. The proposed model trained on 2000 fundus images of high quality from a combination of six public databases: ODIR, Eye Diseases Classification from Kaggle, DR-200, Fundus Dataset, RFMiD, and ARIA. El-Den et al. (2023) proposed an integrated AE model with TL based on using six different pre-trained models (ResNet50, VGG16, ResNet18, Inception-V3, VGG19, and ResNet101) with two different optimizers to differentiate between wet, GA, intermediate grades, and normal retina using a private dataset consisting of 864 CFP. Integration with the ResNet50 pre-trained model using the SGD optimizer recorded the best accuracy of 96.23%, a sensitivity of 96.2%, and a specificity of 99%. Kallel and Kammoun (2024) used SVM to classify CFP into normal, age-related maculopathy, dry AMD, and nAMD with an accuracy of 98.4%, specificity of 100%, the sensitivity of 97.56%, the precision of 100%, F1-score of 98%, AUC of 0.9887, and kappa score of 0.9649 using a dataset from the Habib Bourguiba University Hospital. They employed hybrid human-artificial intelligence (H-AI) to interact continuously and increase human cognitive ability rather than replace it. The left-right contrastive classification (LRCC) pre-processing operation for distinguishing between left and right eye images is considered time consumption. Gour and Khanna (2021) proposed two CNN-based models to perform multi-class multi-label detection for normal retina, AMD, DR, hypertension, myopia, and others. The models were developed using four different pre-trained models: ResNet50, Inception-V3, MobileNet, and VGG16, with two optimizers, Adam and SGD. The VGG16 with the SGD optimizer was the best model, recording an accuracy of 87.16%, AUC of 0.8493, and an F1-score of 85.57%, using a multi-labeled dataset composed of 5000 fundus images for 8 different ophthalmic diseases. Mookiah et al. (2014) proposed an automated AMD detection system to differentiate between the normal retina and different grades of dry AMD (early, intermediate, and advanced) comparing between NB, k-NN, probabilistic neural network (PNN), DT, and SVM classifiers. SVM recorded the highest accuracy of 90.19%, using a private dataset from Kasturba Medical Hospital, Manipal, India, and 95.07% using the ARIA dataset, and 95% using the STARE dataset.

4 Discussion

In this review, we discussed the detection and classification of AMD. Numerous AI-based automated systems and procedures have been developed and explored to analyze the disease's characteristics. We considered all relevant journal articles and conference papers up to June 2024. We selected publications from the past ten years (from 2014 to 2024) on the topic, revealing that AI helped diagnose and grade AMD using different retinal imaging modalities, such as CFP and OCT scans. We gathered the research publications for this review from the most prominent databases based on their accessibility, quality, and availability, such as PubMed, NIH, Web of Science, Google Scholar, and IEEE Xplore. DL-based models utilizing TL methodology are gaining popularity recently, exhibiting impressive results and performance in diagnosing and classifying disease grades and different severity levels using various retinal imaging techniques.

Table 6 Modern research and developments for detecting and identifying AMD grades using Fundus medical imaging modalities

Methodology and references	Dataset (#images)	Performance measurement	Classification	Advantage	Limitation
SVM (Kallel and Kammoun 2024)	Habib Private (377)	Acc.: 98.4% Spec.: 100% Sens.: 97.56% Prec.:100% F1-score: 98% AUC.: 0.9887 kappa: 0.9649	Normal, maculopathy, Dry, and nAMD 4-class	H-AI system merging human intelligence with AI capabilities assuring better performance worthy attempt to broaden H-AI challenges	Limited dataset size, overfitting risk, biased to dataset required high image quality LRCC time consumption
AMDNet23 (Ali et al. 2024)	ODIR DR-200 RFMiD ARIA Fundus DS Eye Diseases Classification (2k)	Acc.: 96.50% Spec.: 99.32% Sens.: 96.5% Pre.: 96.51% F1-score: 96.49%	Normal, AMD, cataract, DR (4-class)	Good performance indicator for detecting different retinal disorder worthy attempt for generalization capability	Biased to dataset imbalance dataset overfitting risk
Autoencoder integrated with ResNet50 (El-Den et al. 2023)	Private (864)	Acc.: 96.23% Spec.: 96.2% Sens.: 99%	GA, wet, intermediate, normal (4-class)	Good performance indicator accepting varying CFP size and detect being GA, wet, intermediate or normal retina automatically	Limited dataset size, risk losing fine feature overfitting risk required high image quality
Ensamble approach to bonding EfficientNet-B0, VGG16, and ResNet152 (Kumar and Singh 2023)	Messidor-2, EyePACS, HRF, DRIVE, ARIA and STARE (20K)	Acc.: 99.71% Sens.: 97.85% Prec.: 98.26% F1-score: 99.21% AUC: 0.9896 kappa: 0.9902	Dry AMD, wet AMD, and other retinal diseases (10-class)	High performance indicator, combine different models to improve performance useful for fast eye-screening for early detection of 10 retinal disorder	High computational cost, architecture complexity, sensitive to poor model require high, image quality
CNN integrated with YOLO-V3 (Dong et al. 2022)	Private(208K)	Acc.:97.3% Spec.: 98% Sens.: 88%	AMD, DR, and other retinal diseases (10-class)	High performance indicator for detecting 10 retinal disorders, save time and resource	Biased to dataset, confront difficulty identifying small object, biased to dataset inadequate to differentiate between AMD grades

Table 6 (continued)

Methodology and references	Dataset (#images)	Performance measurement	Classification	Advantage	Limitation
VGG16 (Gour and Khanna 2021)	Private (5k)	Acc.: 87.16% F1-Score: 85.57% AUC: 0.8493	Normal, AMD, DR, Hypertension and other (Multi-class Multi-lable)	Using TF technique overcome dataset limitation	High computational cost, biased to dataset, large number of parameters, overfitting risk
DCNN (Bhuiyan et al. 2020)	AREDS	Acc.: 96.1% Sens.: 98.9% Spec.: 99.5% AUC.: 0.99 kappa: 0.983	Normal, early, intermediate, and advanced (4-class)	Good performance indicator, no need for extracting features manually	Require high image quality biased to dataset overfitting risk
DeepSeeNet (Peng et al. 2019)	AREDS	Acc.: 67.1% Sens.: 59% Spec.: 93% kappa: 0.558	AMD grades (3-class)	Better performance compared to specialists	Required high image quality, imbalanced dataset, overfitting risk
LSVM (Burlina et al. 2017)	AREDS	Acc.: 81.5% kappa: 0.7226	No or early, intermediate, and advanced AMD (3-class)	Using TF technique to overcome dataset limitation, the model closed to physician	Required high image quality and, fine-tuning, imbalanced dataset, overfitting risk
	AREDS	Acc.: 79.4% kappa: 0.6962	No, early, intermediate, and advanced AMD (4-class)		
SVM classifiers. (Mookiah et al. 2014)	Private (540)	Acc.: 90.19% Sens.: 88.89% Spec.: 91.48%	No, early, intermediate, and advanced AMD (4-class)	Manually extracting features guarantees extracting the most significant and impactful feature	Require larger dataset, large computation resource, biased to dataset, require high image quality
	ARIA (161)	Acc.: 95.07% Sens.: 96.09% Spec.: 93.33%			
	STARE (83)	Acc.: 95% Sens.: 96% Spec.: 93.33%			

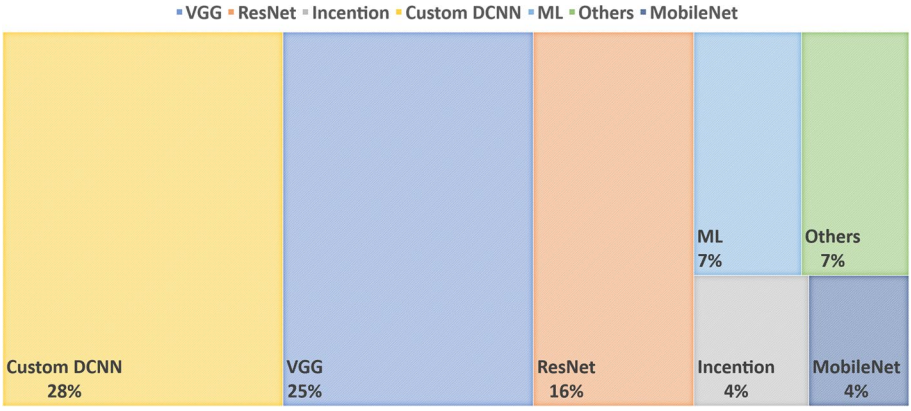

Fig. 6 An illustrative diagram for the used models, including ML, DL, and TL pre-trained models, in AMD detection and classification studies throughout this review

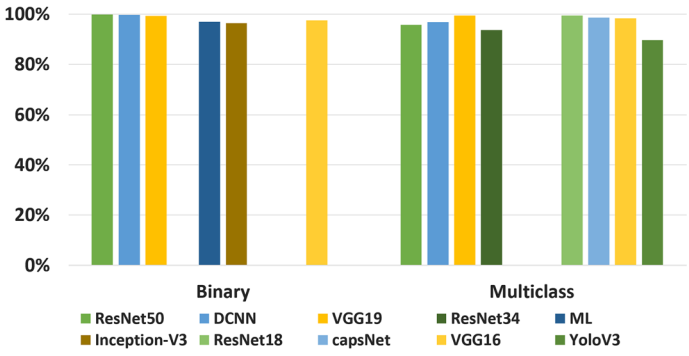

Fig. 7 Highest recorded accuracy of the reviewed publication models in detecting and classifying AMD grading

Based on our literature review, Fig. 6 shows the usability of different AI approaches, including ML, custom CNN, and pre-trained model families, as backbone models for the discussed studies of detecting and prognosis of AMD diseases, demonstrating that DL has advanced over ML, where the VGG-family, including VGG16 and VGG19, recorded 25%, and ResNet-family, including ResNet50, ResNet18, and ResNet152, recorded 16%, while 16% of the studies used ML techniques such as NB, k-NN, LSVM, random forest, and SVM classifiers. Additionally, Inception-Family and other pre-trained models recorded 5% each. Figure 7 shows the highest accuracy recorded using different AI approaches for detecting and classifying AMD grades.

OCT scans are popular for AMD grading; meanwhile, CFP performed well in diagnosing AMD and detecting its grades; however, CFP alone is insufficient for diagnosing nAMD as they underestimate the possible presence of CNV. To improve performance, (Kadry et al. 2022) studies training the VGG16 pre-trained model to detect AMD using OCT scans combined with CFP modalities. Moreover, (Elsharkawy et al. 2024; Yan et al. 2021) were capable of classifying wet AMD into active AMD and inactive AMD using OCT image modality.

Several studies (Burlina et al. 2017; Chakraborty and Pramanik 2022; He et al. 2022; Keel et al. 2019; Lee et al. 2017; Ogundokun et al. 2023; Tan et al. 2018; Thomas et al. 2021; Wang et al. 2020; Wang et al. 2023; Zang et al. 2023) performed binary classification to detect the presence or absence of AMD. (Pečiulis et al. 2021) performed binary classification according to locating AMD's lesion zone.

Some studies (Bhuiyan et al. 2020; Burlina et al. 2017; Chen et al. 2021; Chen et al. 2023) conducted binary and n-class classification. Other studies (Akça et al. 2024; El-Den et al. 2023; Elsharkawy et al. 2024; Han et al. 2022; Mookiah et al. 2014; Serener and Serte 2019; Sotoudeh-Paima et al. 2022; Wang et al. 2020) performed multi-class classification differentiating between AMD different grades.

The reviewed studies relied on various performance metrics, including accuracy, ROC curve, AUC, sensitivity, specificity, precision, kappa score, and F1-score. Furthermore, Bhuiyan et al. (Bhuiyan et al. 2020) proposed a model that is capable of anticipating AMD progression for one and two years, while Pham et al. (2022) attempted to generate predictions of drusen changes over time.

The comparative results indicated that most of the reviewed literature used private OCT datasets to detect and grade AMD. The most commonly used public datasets are Mendely, recording accuracy over 95% for binary and *n*-way classification problems. Some of the reviewed publications used their private dataset for training while testing and evaluating the trained model on a public dataset for detecting and classifying AMD grades. Figure 8 plots the accuracy values of the reviewed publication models used to detect and classify AMD grades using OCT datasets.

Studies that trained their proposed model using a small private dataset, (Kadry et al. 2022; Kallel and Kammoun 2024; Motozawa et al. 2019; Wang et al. 2020), may endure biased and insufficient data limitations, which may lead to overfitting results; hence, it is unclear that their findings can be applied widely. Applying TL using a pre-trained model such as ResNet50, Inception-V3, and VGG16, applying data augmentation, and testing the model using public datasets is recommended. However, (Chen et al. 2021; Chen et al. 2023; El-Den et al. 2023; He et al. 2022; Ogundokun et al. 2023; Oliveira et al. 2024; Pečiulis et al. 2021; Saha et al. 2019; Serener and Serte 2019) there is a possibility that the pre-trained model is extracting features that were not previously identified or overlooked by humans due to training on alternate disciplines. Although TL is recommended to overcome the limitations of DL-based models, VGG-family-based (Chen et al. 2021; ; Gour and Khanna 2021; Han et al. 2022; Sotoudeh-Paima et al. 2022; Wang et al. 2020)models may confront significant time consumption limitations due to the enormous number of parameters despite its simple architecture and high-performance indicators findings.

In disease detection and classification, ML techniques have been widely used, with a predominant focus on articles reporting DL and TL methodologies. These studies have demonstrated the successful detection of AMD in fundus images using various public and private databases.

Based on the outcomes of these studies, we recommend developing fully automated CAD systems using AI-based approaches to detect various ophthalmic diseases. It is important to note that these AI-based models are not intended to replace ophthalmologists but rather serve as facilitating tools in clinical settings. They can significantly expedite the process of determining the grade and severity of illnesses, thereby saving valuable time and resources.

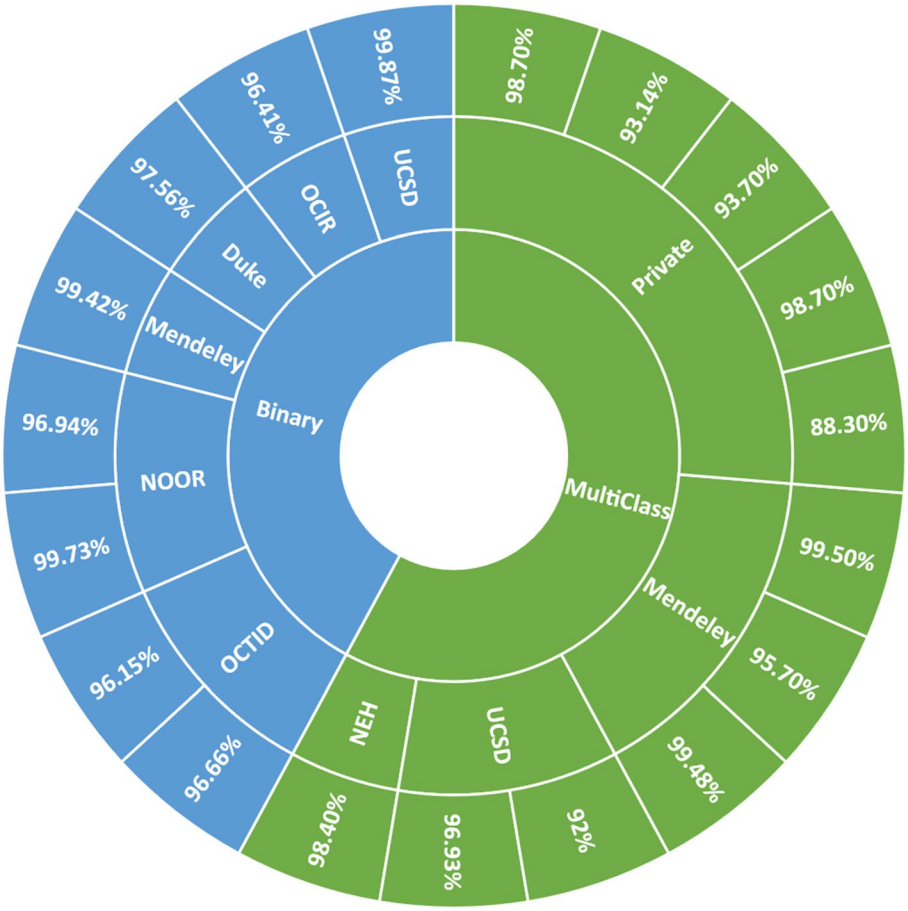

Fig. 8 Accuracy of the reviewed publication models in detecting and classifying AMD grading using public and private OCT datasets

5 Future direction

By integrating AI technology into clinical practice, ophthalmologists can leverage the benefits of these developed models to enhance the accuracy of their diagnostic capabilities and provide more efficient medical care for patients. Many patients suffer from many retinal disorders; hence, developing more advanced intelligent CAD systems for clinical use that can detect and discriminate between different retinal disorders by integrating different imaging modalities, such as OCT with CFP, is important. Future research may investigate the gene for the disease and combine genomic data with imaging techniques.

Witnessing the rapid development of NLP and transformers, studying the recorded medical text and clinical notes may develop an automatic reporting system that generates a sheet with the patient's condition, including the prescribed medication. It is crucial to ensure data security measures to protect patient confidentiality and adhere to AI ethics.

With the presence of self-attention-based models, building a hybrid architecture model combining CNN with ViTs may leverage the strengths of both approaches to develop a robust model with high-performance metrics for CV challenges.

Looking ahead, AI approaches will become increasingly prevalent and vital for retinal disorder screening and assessment, improving the efficiency and accessibility of examinations and enhancing the accuracy of detecting and diagnosing disease severity levels.

6 Conclusion

In conclusion, AI has the potential to accelerate diagnostic procedures, reduce clinician workload, and eliminate diagnostic errors caused by improper data integration. AI can extract characteristics from complicated and diverse imaging modalities, enabling the development of novel biomarkers to expand our current understanding of illnesses. DL and TL pre-trained models have shown remarkable achievements in diagnosing ophthalmic diseases, particularly in image classification using fundus images or OCT scans. The findings from the DL analysis hold great promise for enhancing clinical assessments and improving patient medical care. This could potentially introduce newly discovered diagnostic findings into clinical practice or aid in developing new treatments for retinal disorders.

Author contributions N. NE. & M. E. & I. S.: conceptualization, prepared figures, review methodology, writing original draft preparation. M. G. $ A. K. & M. Z. H.: writing original review preparation, review methodology, writing original draft Preparation. A. S. & H. M. & A. E.: supervision, investigation (execution of review) and writing (review & editing).

Data availability No datasets were generated or analysed during the current study.

Declarations

Conflict of interest The authors declare no conflict of interest.

References

Akça S, Garip Z, Ekinci E, Atban F (2024) Automated classification of choroidal neovascularization, diabetic macular edema, and drusen from retinal OCT images using vision transformers: a comparative study. Lasers Med Sci 39(1):140

Alam TM, Shaukat K, Khan WA, Hameed IA, Almuqren LA, Raza MA, Aslam M, Luo S (2022) An efficient deep learning-based skin cancer classifier for an imbalanced dataset. Diagnostics 12(9):2115

Ali MA, Hossain MS, Hossain MK, Sikder SS, Khushbu SA, Islam M (2024) Amdnet23: Hybrid CNN-LSTM deep learning approach with enhanced preprocessing for age-related macular degeneration (AMD) detection. Intell Syst Appl 21:200334
Almutairi S, Manimurugan S, Kim B-G, Aborokbah MM, Narmatha C (2023) Breast cancer classification using deep Q learning (DQL) and gorilla troops optimization (GTO). Appl Soft Comput 142:110292
Al-Zamil WM, Yassin SA (2017) Recent developments in age-related macular degeneration: a review. Clin Interv Aging 12:1313
Anoop B et al (2022) Binary classification of DR-diabetic retinopathy using CNN with fundus colour images. Mater Today Proc 58:212–216
An G, Yokota H, Motozawa N et al (2019) Deep learning classification models built with two-step transfer learning for age related macular degeneration diagnosis. In: 2019 41st annual international conference of the IEEE Engineering in Medicine and Biology Society (EMBC), pp 2049–2052. IEEE
Apte RS (2021) Age-related macular degeneration. New England J Med 385(6):539–547
AREDS1: [dataset]. National Eye Institute (NEI) Age-related eye disease study (AREDS), dbgap, V1 (2006) https://www.ncbi.nlm.nih.gov/projects/gap/cgi-bin/study.cgi?study_id=phs000001
AREDS2: [dataset]. Age-related eye disease study 2 (AREDS2): a multi-center, randomized trial of Lutein, Zeaxanthin, and Omega-3 long-chain polyunsaturated fatty acids (docosahexaenoic acid [DHA] and eicosapentaenoic acid [EPA]) in age-related macular degeneration, dbgap, V1; 1970. https://www.ncbi.nlm.nih.gov/projects/gap/cgi-bin/study.cgi?study_id=phs002015
ARIA: AMD public dataset: ARIA. http://www.eyecharity.com/aria_online
Arisdakessian C, Poirion O, Yunits B, Zhu X, Garmire LX (2019) Deepimpute: an accurate, fast, and scalable deep neural network method to impute single-cell RNA-seq data. Genome Biol 20:1–14
Asia A-O, Zhu C-Z, Althubiti SA et al (2022) Detection of diabetic retinopathy in retinal fundus images using CNN classification models. Electronics 11(17):2740
Attri I, Awasthi LK, Sharma TP (2024) Machine learning in agriculture: a review of crop management applications. Multimed Tools Appl 83(5):12875–12915
Azizi MM, Abhari S, Sajedi H (2024) Stitched vision transformer for age-related macular degeneration detection using retinal optical coherence tomography images. PloS ONE 19(6):0304943
Bai J, Yang H, Wu C (2023) MLACNN: an attention mechanism-based CNN architecture for predicting genome-wide DNA methylation. Theor Biosci 142(4):359–370
Bank D, Koenigstein N, Giryes R (2020) Autoencoders. arXiv preprint arXiv:2003.05991
Bellemo V, Lim ZW, Lim G, Nguyen QD, Xie Y, Yip MY, Hamzah H, Ho J, Lee XQ, Hsu W et al (2019) Artificial intelligence using deep learning to screen for referable and vision-threatening diabetic retinopathy in Africa: a clinical validation study. Lancet Dig Health 1(1):35–44
Bhuiyan A, Wong TY, Ting DSW et al (2020) Artificial intelligence to stratify severity of age-related macular degeneration (AMD) and predict risk of progression to late AMD. Transl Vis Sci Technol 9(2):25–25
Bilal A, Sun G (2020) Neuro-optimized numerical solution of non-linear problem based on Flierl-Petviashivili equation. SN Appl Sci 2(7):1166
Bilal A, Sun G, Mazhar S (2021) Finger-Vein recognition using a novel enhancement method with convolutional neural network. J Chin Inst Eng 44(5):407–417
Bilal A, Sun G, Mazhar S, Junjie Z (2021) Neuro-optimized numerical treatment of HIV infection model. Int J Biomath 14(05):2150033
Bilal A, Sun G, Li Y, Mazhar S, Khan AQ (2021) Diabetic retinopathy detection and classification using mixed models for a disease grading database. IEEE Access 9:23544–23553
Bilal A, Sun G, Li Y, Mazhar S, Latif J (2022) Lung nodules detection using grey wolf optimization by weighted filters and classification using CNN. J Chin Inst Eng 45(2):175–186
Bilal A, Shafiq M, Fang F, Waqar M, Ullah I, Ghadi YY, Long H, Zeng R (2022) IGWO-IVNet3: Dl-based automatic diagnosis of lung nodules using an improved gray wolf optimization and InceptionNet-v3. Sensors 22(24):9603
Bilal A, Zhu L, Deng A, Lu H, Wu N (2022) Ai-based automatic detection and classification of diabetic retinopathy using U-Net and deep learning. Symmetry 14(7):1427
Bilal A, Liu X, Baig TI, Long H, Shafiq M (2023) Edgesvdnet: 5G-enabled detection and classification of vision-threatening diabetic retinopathy in retinal fundus images. Electronics 12(19):4094
Bilal A, Liu X, Long H, Shafiq M, Waqar M (2023) Increasing crop quality and yield with a machine learning-based crop monitoring system. Comput Mater Continua 76(2):2401–2426
Bilal A, Imran A, Liu X, Liu X, Ahmad Z, Shafiq M, El-Sherbeeny AM, Long H (2024) BC-QNet: a quantum-infused elm model for breast cancer diagnosis. Comput Biol Med 175:108483

Bilal A, Imran A, Baig TI, Liu X, Abouel Nasr E, Long H (2024) Breast cancer diagnosis using support vector machine optimized by improved quantum inspired grey wolf optimization. Sci Rep 14(1):10714
Bilal A, Liu X, Shafiq M, Ahmed Z, Long H (2024) NIMEQ-SACNet: a novel self-attention precision medicine model for vision-threatening diabetic retinopathy using image data. Comput Biol Med 171:108099
Bilal A, Imran A, Baig TI, Liu X, Long H, Alzahrani A, Shafiq M (2024) Improved support vector machine based on CNN-SVD for vision-threatening diabetic retinopathy detection and classification. Plos ONE 19(1):0295951
Bouma BE, Yun S-H, Vakoc BJ et al (2009) Fourier-domain optical coherence tomography: recent advances toward clinical utility. Curr Opin Biotechnol 20(1):111–118
Bourne R, Steinmetz JD, Flaxman S et al (2021) Trends in prevalence of blindness and distance and near vision impairment over 30 years: an analysis for the global burden of disease study. Lancet Global Health 9(2):130–143
Burlina P, Pacheco KD, Joshi N et al (2017) Comparing humans and deep learning performance for grading AMD: a study in using universal deep features and transfer learning for automated AMD analysis. Comput Biol Med 82:80–86
Burlina PM, Joshi N, Pekala M et al (2017) Automated grading of age-related macular degeneration from color fundus images using deep convolutional neural networks. JAMA Ophthalmol 135(11):1170–1176
Caleffi F, Silva Rodrigues L, Silva Stamboroski J, Pereira BM (2024) Small-scale self-driving cars: a systematic literature review. J Traffic Transp Eng. https://doi.org/10.1016/j.jtte.2023.09.005
Carbonell JG, Michalski RS, Mitchell TM (1983) An overview of machine learning. Mach Learn. https://doi.org/10.1016/B978-0-08-051054-5.50005-4
Celebi ARC, Bulut E, Sezer A (2023) Artificial intelligence based detection of age-related macular degeneration using optical coherence tomography with unique image preprocessing. Eur J Ophthalmol 33(1):65–73
Chakraborty R, Pramanik A (2022) DCNN-based prediction model for detection of age-related macular degeneration from color fundus images. Med Biol Eng Comput 60(5):1431–1448
Chan H-P, Samala RK, Hadjiiski LM et al (2020) Deep learning in medical image analysis. Springer, Berlin
Chen Y-M, Huang W-T, Ho W-H et al (2021) Classification of age-related macular degeneration using convolutional-neural-network-based transfer learning. BMC Bioinform 22(5):1–16
Chen X, Xue Y, Wu X et al (2023) Deep learning-based system for disease screening and pathologic region detection from optical coherence tomography images. Transl Vis Sci Technol 12(1):29–29
Ciardella AP, Donsoff IM, Huang SJ et al (2004) Polypoidal choroidal vasculopathy. Surv Ophthalmol 49(1):25–37
Clemons TE, Chew EY, Bressler SB, McBee W et al (2003) National Eye Institute visual function questionnaire in the age-related eye disease study (AREDS): AREDS report no. 10. Arch Ophthalmol 121(2):211–217
Creswell A, White T, Dumoulin V, Arulkumaran K, Sengupta B, Bharath AA (2018) Generative adversarial networks: an overview. IEEE Signal Process Mag 35(1):53–65
Dansingani K, Naysan J, Freund K (2015) En face OCT angiography demonstrates flow in early type 3 neovascularization (retinal angiomatous proliferation). Eye 29(5):703–706
Deng Y, Qiao L, Du M et al (2022) Age-related macular degeneration: epidemiology, genetics, pathophysiology, diagnosis, and targeted therapy. Genes Dis 9(1):62–79
Di Carlo E, Augustin AJ (2021) Prevention of the onset of age-related macular degeneration. J Clin Med 10(15):3297
Diao S, Su J, Yang C et al (2023) Classification and segmentation of oct images for age-related macular degeneration based on dual guidance networks. Biomed Signal Process Control 84:104810
Dong L, Yang Q, Zhang RH et al (2021) Artificial intelligence for the detection of age-related macular degeneration in color fundus photographs: a systematic review and meta-analysis. EclinicalMedicine 35:100875
Dong L, He W, Zhang R et al (2022) Artificial intelligence for screening of multiple retinal and optic nerve diseases. JAMA Netw Open 5(5):229960–229960
Dosovitskiy A, Beyer L, Kolesnikov A, Weissenborn D, Zhai X, Unterthiner T, Dehghani M, Minderer M, Heigold G, Gelly S et al (2020) An image is worth 16x16 words: transformers for image recognition at scale. arXiv preprint arXiv:2010.11929
El-Den NN, Naglah A, Elsharkawy M et al (2023) Scale-adaptive model for detection and grading of age-related macular degeneration from color retinal fundus images. Sci Rep 13(1):9590

Elkorany AS, Elsharkawy ZF (2023) Efficient breast cancer mammograms diagnosis using three deep neural networks and term variance. Sci Rep 13(1):2663
Elkorany AS, Marey M, Almustafa KM, Elsharkawy ZF (2022) Breast cancer diagnosis using support vector machines optimized by whale optimization and dragonfly algorithms. IEEE Access 10:69688–69699
Elsharkawy M, Sharafeldeen A, Taher F, Shalaby A, Soliman A, Mahmoud A, Ghazal M, Khalil A, Alghamdi NS, Razek AAKA et al (2021) Early assessment of lung function in coronavirus patients using invariant markers from chest X-rays images. Sci Rep 11(1):12095
Elsharkawy M, Elrazzaz M, Ghazal M et al (2021) Role of optical coherence tomography imaging in predicting progression of age-related macular disease: a survey. Diagnostics 11(12):2313
Elsharkawy M, Sharafeldeen A, Soliman A et al (2022) A novel computer-aided diagnostic system for early detection of diabetic retinopathy using 3D-OCT higher-order spatial appearance model. Diagnostics 12(2):461
Elsharkawy M, Elrazzaz M, Sharafeldeen A, Alhalabi M, Khalifa F, Soliman A, Elnakib A, Mahmoud A, Ghazal M, El-Daydamony E et al (2022) The role of different retinal imaging modalities in predicting progression of diabetic retinopathy: a survey. Sensors 22(9):3490
Elsharkawy M, Soliman A, Mahmoud A, Ghazal M, Alhalabi M, El-Baz A, Thanos A, Sandhu HS, Giridharan G, El-Baz A (2023) Prevention of age-related macular degeneration disease: current strategies and future directions. Photo acoustic and optical coherence tomography imaging, volume 1: diabetic retinopathy. IOP Publishing Bristol, Bristol, pp 1–13
Elsharkawy M, Sharafeldeen A, Khalifa F, Soliman A, Elnakib A, Ghazal M, Sewelam A, Thanos A, Sandhu H, El-Baz A (2024) A clinically explainable AI-based grading system for age-related macular degeneration using optical coherence tomography. IEEE J Biomed Health Inform. https://doi.org/10.1109/JBHI.2024.3355329
Elsharkawy M, Sharafeldeen A, Soliman A et al (2022) Diabetic retinopathy diagnostic cad system using 3d-oct higher order spatial appearance model. In: 2022 IEEE 19th international symposium on biomedical imaging (ISBI), pp 1–4. IEEE
Feng X, Xiu Y-H, Long H-X, Wang Z-T, Bilal A, Yang L-M (2024) Advancing single-cell RNA-seq data analysis through the fusion of multi-layer perceptron and graph neural network. Brief Bioinform 25(1):481
Ferris FL, Davis MD, Clemons TE et al (2005) A simplified severity scale for age-related macular degeneration: AREDS report no. 18. Arch Ophthalmol (Chicago, Ill.: 1960) 123(11):1570–1574
Ferris FL III, Wilkinson C, Bird A, Chakravarthy U, Chew E, Csaky K, Sadda SR et al (2013) Clinical classification of age-related macular degeneration. Ophthalmology 120(4):844–851
Fleckenstein M, Keenan TD, Guymer RH et al (2021) Age-related macular degeneration. Nat Rev Dis Primers 7(1):31
Fletcher DC, Schuchard RA, Renninger LW (2012) Patient awareness of binocular central scotoma in age-related macular degeneration. Optom Vis Sci 89(9):1395–1398
Flores R, Carneiro Â, Tenreiro S et al (2021) Retinal progression biomarkers of early and intermediate age-related macular degeneration. Life 12(1):36
Gehrs KM, Anderson DH, Johnson LV et al (2006) Age-related macular degeneration-emerging pathogenetic and therapeutic concepts. Ann Med 38(7):450–471
Gholami P, Roy P, Parthasarathy MK et al (2020) OCTID: optical coherence tomography image database. Comput Electr Eng 81:106532
Gour N, Khanna P (2021) Multi-class multi-label ophthalmological disease detection using transfer learning based convolutional neural network. Biomed Signal Process Control 66:102329
Gueddena Y, Aboudi N, Zgolli H, Mabrouk S, Sidibe D, Tabia H, Khlifa N (2024) A new intelligent system based deep learning to detect DME and AMD in OCT images. Int Ophthalmol 44(1):191
Haggag S, Elnakib A, Sharafeldeen A et al (2022) A computer-aided diagnostic system for diabetic retinopathy based on local and global extracted features. Appl Sci 12(16):8326
Han J, Choi S, Park JI et al (2022) Classifying neovascular age-related macular degeneration with a deep convolutional neural network based on optical coherence tomography images. Sci Rep 12(1):2232
Hassan T, Akram MU, Masood MF et al (2019) Deep structure tensor graph search framework for automated extraction and characterization of retinal layers and fluid pathology in retinal SD-OCT scans. Comput Biol Med 105:112–124
He T, Zhou Q, Zou Y (2022) Automatic detection of age-related macular degeneration based on deep learning and local outlier factor algorithm. Diagnostics 12(2):532
Hearst MA, Dumais ST, Osuna E, Platt J, Scholkopf B (1998) Support vector machines. IEEE Intell Syst Their Appl 13(4):18–28
Hernández-Zimbrón LF, Zamora-Alvarado R, Velez-Montoya R et al (2018) Age-related macular degeneration: new paradigms for treatment and management of AMD. Oxid Med Cell Longev 2018:8374647

He K, Zhang X, Ren S, Sun J (2016) Deep residual learning for image recognition. In: Proceedings of the IEEE conference on computer vision and pattern recognition, pp 770–778
Hobbs SD, Pierce K (2022) Wet age-related macular degeneration (wet amd). In: StatPearls. StatPearls Publishing
Howard A, Sandler M, Chu G, Chen L-C, Chen B, Tan M, Wang W, Zhu Y, Pang R, Vasudevan V et al (2019) Searching for mobilenetv3. In: Proceedings of the IEEE/CVF international conference on computer vision, pp. 1314–1324
Hussain Ali Y, Sabu Chooralil V, Balasubramanian K, Manyam RR, Kidambi Raju S (2023) Optimization system based on convolutional neural network and internet of medical things for early diagnosis of lung cancer. Bioengineering 10(3):320
Hwang DD-J, Choi S, Ko J, Yoon J, Park JI, Hwang JS, Han JM, Lee HJ, Sohn J, Park KH et al (2021) Distinguishing retinal angiomatous proliferation from polypoidal choroidal vasculopathy with a deep neural network based on optical coherence tomography. Sci Rep 11(1):9275
iChallenge-AMD: AMD public dataset: iChallenge-AMD. http://ai.baidu.com/broad/introduction
Ipp E, Liljenquist D, Bode B, Shah VN, Silverstein S, Regillo CD, Lim JI, Sadda S, Domalpally A, Gray G et al (2021) Pivotal evaluation of an artificial intelligence system for autonomous detection of referrable and vision-threatening diabetic retinopathy. JAMA Netw Open 4(11):2134254–2134254
Kadry S, Rajinikanth V, González Crespo R et al (2022) Automated detection of age-related macular degeneration using a pre-trained deep-learning scheme. J Supercomput. https://doi.org/10.1371/journal.pone.0284060
Kallel IF, Kammoun S (2024) Hybrid human-artificial intelligence system for early detection and classification of AMD from fundus image. Signal Image Video Process 18(5):4779–4796
Keel S, Li Z, Scheetz J et al (2019) Development and validation of a deep-learning algorithm for the detection of neovascular age-related macular degeneration from colour Fundus photographs. Clin Exp Ophthalmol 47(8):1009–1018
Keenan TD, Dharssi S, Peng Y et al (2019) A deep learning approach for automated detection of geographic atrophy from color Fundus photographs. Ophthalmology 126(11):1533–1540
Khan AQ, Sun G, Khalid M, Imran A, Bilal A, Azam M, Sarwar R (2024) A novel fusion of genetic grey wolf optimization and kernel extreme learning machines for precise diabetic eye disease classification. Plos ONE 19(5):0303094
Klein R, Klein BE, Tomany SC et al (2002) Ten-year incidence and progression of age-related maculopathy: the beaver dam eye study. Ophthalmology 109(10):1767–1779
Klein R, Klein BE, Knudtson MD et al (2007) Fifteen-year cumulative incidence of age-related macular degeneration: the beaver dam eye study. Ophthalmology 114(2):253–262
Kumar KS, Singh NP (2023) Retinal disease prediction through blood vessel segmentation and classification using ensemble-based deep learning approaches. Neural Comput Appl 35(17):12495–12511
Le PH, Patel BC (2020) Optical coherence tomography angiography
Lee SM, Lee D (2020) Healthcare wearable devices: an analysis of key factors for continuous use intention. Serv Bus 14(4):503–531
Lee D, Yoon SN (2021) Application of artificial intelligence-based technologies in the healthcare industry: opportunities and challenges. Int J Environ Res Public Health 18(1):271
Lee CS, Baughman DM, Lee AY (2017) Deep learning is effective for classifying normal versus age-related macular degeneration oct images. Ophthalmol Retina 1(4):322–327
Leingang O, Riedl S, Mai J et al (2023) Automated deep learning-based AMD detection and staging in real-world OCT datasets (pinnacle study report 5). Sci Rep 13(1):19545
Lim LS, Mitchell P, Seddon JM et al (2012) Age-related macular degeneration. Lancet 379(9827):1728–1738
Li S, Quan Z (2020) Attention-aware convolutional neural network for age-related macular degeneration classification. In: 2020 12th international conference on communication software and networks (ICCSN), pp. 264–269. IEEE
Maguire MG, Martin DF, Ying G-s, Jaffe GJ, Daniel E, Grunwald JE, Toth CA, Ferris FL III, Fine SL et al (2016) Five-year outcomes with anti-vascular endothelial growth factor treatment of neovascular age-related macular degeneration: the comparison of age-related macular degeneration treatments trials. Ophthalmology 123(8):1751–1761
Mahmoudi Z, DelFavero S, Jacob P, Choudhary P et al (2021) Toward an optimal definition of hypoglycemia with continuous glucose monitoring. Comput Methods Prog Biomed 209:106303
Menke MN, Dabov S, Sturm V (2008) Features of age-related macular degeneration assessed with three-dimensional fourier-domain optical coherence tomography. Br J Ophthalmol 92(11):1492–1497
Mitchell P, Liew G, Gopinath B et al (2018) Age-related macular degeneration. Lancet 392(10153):1147–1159

Mohan NJ, Murugan R, Goel T, Roy P (2023) DRFL: federated learning in diabetic retinopathy grading using fundus images. IEEE Trans Parallel Distrib Syst. https://doi.org/10.1109/TPDS.2023.3264473
Mookiah MRK, Acharya UR, Koh JE et al (2014) Automated diagnosis of age-related macular degeneration using greyscale features from digital Fundus images. Comput Biol Med 53:55–64
Motozawa N, An G, Takagi S et al (2019) Optical coherence tomography-based deep-learning models for classifying normal and age-related macular degeneration and exudative and non-exudative age-related macular degeneration changes. Ophthalmol Ther 8:527–539
Naseer I, Akram S, Masood T, Rashid M, Jaffar A (2023) Lung cancer classification using modified U-Net based lobe segmentation and nodule detection. IEEE Access 11:60279
National Institutes of Health: Age-Related Macular Degeneration (AMD) (2021) National Eye Institute (NEI). Accessed 21 Jun 2021
NOOR: Noor Eye Hospital in Tehran. https://hrabbani.site123.me/available-datasets/dataset-for-oct-classification-50-normal-48-amd-50-dme
Ogundokun RO, Abdulahi AT, Adenike AR et al (2023) Inception v3 based approach for the recognition of age-related macular degeneration disease. In: 2023 international conference on science, engineering and business for sustainable development goals (SEB-SDG), vol. 1, pp 1–7. IEEE
Oliveira GC, Rosa GH, Pedronette DC, Papa JP, Kumar H, Passos LA, Kumar D (2024) Robust deep learning for eye fundus images: bridging real and synthetic data for enhancing generalization. Biomed Signal Process Control 94:106263
Ongsulee P (2017) Artificial intelligence, machine learning and deep learning. In: 2017 15th international conference on ICT and knowledge engineering (ICT &KE), pp 1–6. IEEE
Pečiulis R, Lukoševičius M, Kriščiukaitis A et al (2021) Automated age-related macular degeneration area estimation–first results. arXiv preprint arXiv:2107.02211
Peng Y, Dharssi S, Chen Q et al (2019) Deepseenet: a deep learning model for automated classification of patient-based age-related macular degeneration severity from color Fundus photographs. Ophthalmology 126(4):565–575
Peterson LE (2009) K-nearest neighbor. Scholarpedia 4(2):1883
Pham QT, Ahn S, Shin J et al (2022) Generating future fundus images for early age-related macular degeneration based on generative adversarial networks. Comput Methods Prog Biomed 216:106648
Polito A, Napolitano M, Bandello F et al (2006) The role of optical coherence tomography (OCT) in the diagnosis and management of retinal angiomatous proliferation (RAP) in patients with age-related macular degeneration. Ann Acad Med Singapore 35(6):420
Raja MAZ, Khan JA, Zameer A, Khan NA, Manzar MA (2019) Numerical treatment of nonlinear singular Flierl-Petviashivili systems using neural networks models. Neural Comput Appl 31:2371–2394
Rasti R, Rabbani H, Mehridehnavi A et al (2017) Macular OCT classification using a multi-scale convolutional neural network ensemble. IEEE Trans Med Imaging 37(4):1024–1034
Redmon J, Farhadi A (2018) Yolov3: an incremental improvement. arXiv preprint arXiv:1804.02767
Regatieri CV, Branchini L, Duker JS (2011) The role of spectral-domain OCT in the diagnosis and management of neovascular age-related macular degeneration. Ophthalmic Surg Lasers Imaging Retina 42(4):56–66
Rein DB, Wittenborn JS, Burke-Conte Z et al (2022) Prevalence of age-related macular degeneration in the US in 2019. JAMA Ophthalmol 140(12):1202–1208
Rish I et al (2001) An empirical study of the naive bayes classifier. In: IJCAI 2001 workshop on empirical methods in artificial intelligence, vol. 3, pp 41–46. Citeseer
Sabir Z, Said SB, Al-Mdallal Q (2024) Artificial intelligent solvers for the HIV-1 system including aids based on the cancer cells. Intell Syst Appl 21:200309
Saha S, Nassisi M, Wang M et al (2019) Automated detection and classification of early AMD biomarkers using deep learning. Sci Rep 9(1):10990
Sahoo M, Mitra M, Pal S (2023) Improved detection of dry age-related macular degeneration from optical coherence tomography images using adaptive window based feature extraction and weighted ensemble based classification approach. Photodiagnosis Photodyn Ther 42:103629
Saleh GA, Batouty NM, Haggag S, Elnakib A, Khalifa F, Taher F, Mohamed MA, Farag R, Sandhu H, Sewelam A et al (2022) The role of medical image modalities and AI in the early detection, diagnosis and grading of retinal diseases: a survey. Bioengineering 9(8):366
Salehinejad H, Sankar S, Barfett J, Colak E, Valaee S (2017) Recent advances in recurrent neural networks. arXiv preprint arXiv:1801.01078
Sandhu HS, Elmogy M, Sharafeldeen AT et al (2020) Automated diagnosis of diabetic retinopathy using clinical biomarkers, optical coherence tomography, and optical coherence tomography angiography. Am J Ophthalmol 216:201–206

Schwartz R, Loewenstein A (2015) Early detection of age related macular degeneration: current status. Int JRetina Vitreous 1(1):1–8
Serener A, Serte S (2019) Dry and wet age-related macular degeneration classification using oct images and deep learning. In: 2019 scientific meeting on electrical-electronics & biomedical engineering and computer science (EBBT), pp 1–4. IEEE
Sharafeldeen A, Elsharkawy M, Khalifa F et al (2021) Precise higher-order reflectivity and morphology models for early diagnosis of diabetic retinopathy using OCT images. Sci Rep 11(1):4730
Simonyan K, Zisserman A (2014) Very deep convolutional networks for large-scale image recognition. arXiv preprint arXiv:1409.1556
Sleman AA, Soliman A, Elsharkawy M, Giridharan G, Ghazal M, Sandhu H, Schaal S, Keynton R, Elmaghraby A, El-Baz A (2021) A novel 3D segmentation approach for extracting retinal layers from optical coherence tomography images. Med Phys 48(4):1584–1595
Song Y-Y, Ying L (2015) Decision tree methods: applications for classification and prediction. Shanghai Arch Psychiatry 27(2):130
Sotoudeh-Paima S, Jodeiri A, Hajizadeh F et al (2022) Multi-scale convolutional neural network for automated AMD classification using retinal OCT images. Comput Biol Med 144:105368
Srinivasan PP, Kim LA, Mettu PS et al (2014) Fully automated detection of diabetic macular edema and dry age-related macular degeneration from optical coherence tomography images. Biomed Optics Exp 5(10):3568–3577
Stahl A (2020) The diagnosis and treatment of age-related macular degeneration. Deutsches Ärzteblatt Int 117(29–30):513
STARE: AMD public dataset: STARE. https://cecas.clemson.edu/~ahoover/stare/
Steinmetz JD, Bourne RR, Briant PS et al (2021) Causes of blindness and vision impairment in 2020 and trends over 30 years, and prevalence of avoidable blindness in relation to vision 2020: the right to sight: an analysis for the global burden of disease study. Lancet Global Health 9(2):144–160
Suresh S, Mohan S (2022) NROI based feature learning for automated tumor stage classification of pulmonary lung nodules using deep convolutional neural networks. J King Saud Univ Comput Inform Sci 34(5):1706–1717
Szegedy C, Liu W, Jia Y, Sermanet P, Reed S, Anguelov D, Erhan D, Vanhoucke V, Rabinovich A (2015) Going deeper with convolutions. In: Proceedings of the IEEE conference on computer vision and pattern recognition, pp. 1–9
Takhchidi H, Gliznitsa P, Svetozarskiy S et al (2021) Labelling of data on fundus color pictures used to train a deep learning model enhances its macular pathology recognition capabilities. Bull Russian State Med Univ 4:28–33
Tan JH, Bhandary SV, Sivaprasad S et al (2018) Age-related macular degeneration detection using deep convolutional neural network. Fut Gener Comput Syst 87:127–135
Tang Y (2013) Deep learning using linear support vector machines. arXiv preprint arXiv:1306.0239
Thomas A, Harikrishnan P, Krishna AK et al (2021) A novel multiscale convolutional neural network based age-related macular degeneration detection using OCT images. Biomed Signal Process Control 67:102538
Thomas CJ, Mirza RG, Gill MK (2021) Age-related macular degeneration. Med Clin 105(3):473–491
Thornton J, Edwards R, Mitchell P et al (2005) Smoking and age-related macular degeneration: a review of association. Eye 19(9):935–944
Umar M, Sabir Z, Raja MAZ, Baskonus HM, Yao S-W, Ilhan E (2021) A novel study of Morlet neural networks to solve the nonlinear HIV infection system of latently infected cells. Results Phys 25:104235
Vani MS, Girinath S, Hemasree V, Havardhan LH, Sandhya P (2023) Plant disease identification tracking and forecasting using machine learning. In: 2023 3rd international conference on technological advancements in computational sciences (ICTACS), pp 1428–1432. IEEE
Victor AA (2019) The role of imaging in age-related macular degeneration. Visual impairment and blindness-what we know and what we have to know
Wang MH (2023) An explainable artificial intelligence-based robustness optimization approach for age-related macular degeneration detection based on medical IOT systems. Electronics 12(12):2697
Wang Y, Zhong Y, Zhang L et al (2022) Global incidence, progression, and risk factors of age-related macular degeneration and projection of disease statistics in 30 years: a modeling study. Gerontology 68(7):721–735
Wang Y, Lucas M, Furst J et al (2020) Explainable deep learning for biomarker classification of oct images. In: 2020 IEEE 20th international conference on bioinformatics and bioengineering (BIBE), pp 204–210. IEEE

Wang Y, Ma X, Weddell R et al (2020) Detecting age-related macular degeneration (AMD) biomarker images using MFCC and texture features. In: Medical Imaging 2020: computer-aided diagnosis, vol. 11314, pp 1003–1010. SPIE

Wong WL, Su X, Li X, Cheung CMG et al (2014) Global prevalence of age-related macular degeneration and disease burden projection for 2020 and 2040: a systematic review and meta-analysis. Lancet Global Health 2(2):106–116

Wongchaisuwat P, Thamphithak R, Jitpukdee P et al (2022) Application of deep learning for automated detection of polypoidal choroidal vasculopathy in spectral domain optical coherence tomography. Transl Vis Sci Technol 11(10):16–16

Yan Y, Jin K, Gao Z et al (2021) Attention-based deep learning system for automated diagnoses of age-related macular degeneration in optical coherence tomography images. Med. Phys. 48(9):4926–4934

Yoon SN, Lee D (2018) Artificial intelligence and robots in healthcare: what are the success factors for technology-based service encounters?. Int J Healthc Manag. https://doi.org/10.1080/20479700.2018.1498220

Yu X, Ren J, Long H, Zeng R, Zhang G, Bilal A, Cui Y (2024) iDNA-OpenPrompt: OpenPrompt learning model for identifying DNA methylation. Front Genet 15:1377285

Zang P, Hormel TT, Hwang TS et al (2023) Deep-learning-aided diagnosis of diabetic retinopathy, age-related macular degeneration, and glaucoma based on structural and angiographic OCT. Ophthalmol Sci 3(1):100245

Zapata MA, Royo-Fibla D, Font O et al (2020) Artificial intelligence to identify retinal fundus images, quality validation, laterality evaluation, macular degeneration, and suspected glaucoma. Clin Ophthalmol 14:419–429

Zheng Z, Le NQK, Chua MCH (2023) MaskDNA-PGD: an innovative deep learning model for detecting DNA methylation by integrating mask sequences and adversarial PGD training as a data augmentation method. Chemom Intell Lab Syst 232:104715